PEOPLE'S DEMOCRATIC REPUBLIC OF ALGERIA
Ministry of Higher Education and Scientific Research
MOHAMED BOUDIAF UNIVERSITY - M'SILA

FACULTY OF TECHNOLOGY
FIELD: ELECTONICS
DEPARTEMENT: ELECTRONICS
OPTION: Microelectronics
N°:

Thesis presented for obtaining

Academic Master's degree

By:

Kouici Haroun

Kouici Akram

Title

Design and simulation of photonic crystal sensor based on waveguide coupled cavity for environmental monitoring

Defended before the jury composed of:

Pr. HOCINI Abdesselam	President	Univ. M'sila
Dr. HARHOUZ Ahlam	Supervisor	Univ. M'sila
Dr. TAYOUB Hadjira	Co-Supervisor	URMM/CRTI.Annaba
Dr. Farida KEBAILI	Examiner	Univ. M'sila

JUN. 2023/2024

Acknowledgements

***I** would like to express my deep gratitude to my thesis supervisor, Professor ahlam HARHOUZ, for his supervision, guidance, and continuous support throughout the preparation of this thesis.*

***I** would also like to thank my co-supervisors, Dr Tayoub hadjira, for their time, patience, support, and motivation.*

***I** also express my deep gratitude to Professor HOCINI Abdesselam , professor at M'sila University, for his interest in my work and the honor of chairing the defense committee.*

***I** would like to extend my sincere thanks to the examiner: Dr Farida KEBAILI , professor at M'sila University, for her interest in my work and for agreeing to examine my thesis by participating in the jury.*

for her interest in my work and for agreeing to examine my thesis by participating in the jury. Thank you all for your invaluable support and guidance.

Thank you all for your invaluable support and guidance.

Dédicaces

By the grace of God, the Merciful, the Compassionate, and the Compassionate

I cannot find the right words to express my thanks and gratitude to everyone who has supported me and stood by me during my academic journey. I would like to start by thanking my beloved family, especially my father and mother who have been a strong pillar and a constant source of encouragement and support all these years. To my family members Nourelhouda, Oussama, Fares, Kholoud, Hibetelrahman, and my grand mathers and my fiancée

To my dear friends, who have been by my side in every situation, encouraging me, supporting me, sharing my joys and sorrows, you have been my true companions, and have contributed greatly to making this journey possible and full of beautiful memories.

Finally, to everyone who stood by my side in word and deed, regardless of the distance that separates us, you are an integral part of this achievement. Thank you for sharing my joy and for your continued and invaluable support.

At the end of this wonderful journey, I am deeply grateful and hope that this achievement will be a positive addition to my life and the lives of those around me.

All the best AKRAM

In the name of God, the Merciful, the Compassionate

To the spirits of knowledge and determination, to the moments that shaped us and brightened our thoughts, I dedicate this graduation note. To my mom and dad, who have always been a strong pillar in my life, thank you for your countless support and love. To my brothers and sisters, you are my friends who have shared my beautiful moments and challenges. To my dear professors, who have inspired me and influenced my formation, you are the stars who have lit the way for me. To my friends, who have always been by my side, you are the family I have chosen. I hope that this memorandum will be the end of my university career and the beginning of a bright future. With pride and gratitude.

HAROUN

Contents

General Introduction **8**
Chapter I: Optical Nano-Sensor for Environmental Monitoring: Fundamental Application **10**
I.1 Introduction 11
I.2 Optical sensor technology 11
I.2.1 Nanostructure-Based Sensors **11**
I.2.2 Optical Chemical Sensors **11**
I.2.3 Photonic Crystal Fiber Sensors **12**
I.2.4 Optical biosensors **133**
I.2.5 Optical fiber-based gas sensors **14**
I.2.6 Optical waveguide-based gas sensors **16**
I.3 Types of Environmental Monitoring Optical Sensors 18
I.3.1 Toxic gas monitoring sensors **18**
I.3.2 Water quality monitoring sensors **18**
I.3.3 Indoor environment monitoring **19**
I.3.4 Natural disaster monitoring **19**
I.4 Environmental monitoring applications 19
I.4.1 Volatile organic compounds monitoring **20**
I.4.2 Organ-phosphorus compounds monitoring **23**
I.4.3 Heavy metal ions monitoring **23**
I.4.4 Endocrine disrupting chemicals monitoring **24**
I.5 Photonic crystal chemical sensors for environmental monitoring 24
I.5.1 Definition **24**
I.5.2 Fabrication of the photonic crystal based optical chemical sensor **25**
I.5.3 Surface analysis of the photonic crystal using atomic force microscopy **25**
I.5.4 Colorimetric detection of BTX using the photonic crystal based optical chemical sensor **25**
I.5.5 Characteristics of the photonic crystal based optical chemical sensor **26**
I.5.6 Colorimetric detection of organic solvents using the photonic crystal based optical chemical sensor **277**
I.6 Conclusion 27
Refrences 28
Chapter II: Photonic crystals: Analysis, design and sensing applications **34**
II.1 Introduction 35
II.2 Photonic crystals: Past, present and future 35
II.3 Concepts of Photonic Crystal 36

II.3.1 Periodic Structure and Dimensionality **36**
II.3.2 Photonic Band Gaps and Wave Propagation **37**
II.3.3 Interaction with Electromagnetic Waves **37**
II.4 Modelling of Photonic Structures 38
II.4.1 The plane wave expansion method (PWM) **38**
II.4.2 Finite-difference time-domain method (FDTD) **38**
II.4.3 Boundary conditions (PML) **40**
II.5 Fabrication Process 411
II.5.1 Silicon-On-Insulator (SOI) Platform **411**
II.5.2 Wafer chip preparation **43**
II.5.3 Device Patterning **45**
II.5.4 Process flow for fabrication of alignment markers **455**
II.6 Application of PhCs 466
II.6 .1 Photonic crystal waveguide (PhCW) **466**
II.6 .2 PhC cavities (PhCC) **477**
II.6 .3 Optical properties and sensing principles of PhCCs **477**
II.6 .4 Optical sensors based on PhCs **49**
II.6 .4 .1 PhCW sensors **49**
II.6 .4 .2 Gas sensors based on PhCs **49**
II.6 .4 .3 Refractive index sensor based on PhCs **50**
II.6 .4 .4 Surface wave sensor based on PhCs **52**
II.6 .4 .5 Biochemical sensors based on PhCs **522**
II.6 .4 .6 Temperature sensor based on PhCs **533**
II.6 .4 .7 Oil sensor based on PhCs **533**
II.6.4 .8 Humidity sensor based on PhCs **543**
II.7 Conclusion 544
Refrences 55
Chapter III: Results and discussions **58**
III.1. Introduction 59
III.2. Mechanism detection of Toxic Gas sensor based on Photonic Crystal stucture 59
III. 3. Mathematical background and proposed design 60
III. 3.1. Mathematical background **60**
III. 3.2. The basic structure of the proposed gas sensor 61
III. 3. 3. Gas sensors based on waveguide coupled with cavity **62**
III.4. Results and discussions 666
III.4.1 Study of proposed sensor **66**
III.4.2 Slot geometric parameters effect **68**

III.4.3 Optimized sensor 72
III.4.4 Application: Toxic gaz sensor 73
III.5. Conclusion 74
References 755
General Conclusion 76

List of Figures

Figure. I. 1 Schematic representation of the composition and function of an optical chemical sensor**. 12**
Figure. I. 2A photonic crystal structure interacting with light**. 13**
Figure. I. 3 Schematic representation of the Optical biosensors**. 14**
Figure. I. 4HC-PCF-based gas sensor, (a) schematic of MZI developed using a small stub of HC-PCF, (b) experimental schematic for sensor characterization and interrogation, (c) the response of thesensor to CO2 gas concentration, (d) the response of the sensor to time **16**
Figure. I. 5 Recently proposed waveguide-based gas sensors, (a) schematic view of the gas sensor measuring setup , (b) experimental realization of the gas cell [, (c) schematic of the polarization independent hybrid plasmonic waveguide for gas sensing **. 18**
Figure. I. 6(a) PDMS-coated FBG sensor schematic diagram , (b) sensor spectral response for each VOC **. 22**
Figure. I. 7 Theoretical schematic illustration of the photonic crystal**. 26**
Figure. I. 8 Optical characteristics of photonic crystal based optical**. 26**
Figure. I. 9 Change in the optical characteristics due to the introduction of xylene**. 27**

Figure II 1 Representation of one, two, and three-dimensional photonic crystals. **37**
Figure II 2 Diagram of a Yee cell (3D FDTD discretization). The electric field vectors E are positioned on the edges and the magnetic field vectors H at the center of the faces of the cell. (Vitale, 2014)..... **39**
Figure II 3 Use of PML layers (a) in the 2D case (b) Example of a mesh of a circular structure with application of PML boundary conditions **41**
Figure II 4 Crystal Growth Efficiency with Fluidized Bed Reactor-Produced Granular Polysilicon**. . 43**
Figure II 5 shoulder..... **43**
Figure II 6 The Czochralski method **. 44**
Figure II 7 A/Simulated band diagram for W1 straight PhCW and the corresponding supercell Inset show the magnetic-like field profiles for (a) odd mode and (b) even mode. B/A 90◦ PhC waveguide bend in a finite PhC consisting of circular dielectric rods on a square l **47**
Figure II 8 Schematic structures of (a) L4 PhCC, (b) H0 PhCC, (c) mode-gap PhCC, (d) ring hCC, and (e) shoulder-coupled PhCC **. 48**
Figure II 9 Resonance wavelength shift corresponding to two different indices; n = 1.4000 and n = 1.4480. the resonance is highly sensitive to the refractive index of the fluids over the PhC and this involves a rapid change of the peak position **51**
Figure II 10 Band Structure of TE polarization. The light lines for glass and vacuum at the angle of incidence of 85° are given by lower and upper dashed lines, respectively. The area limited by these lines presents the region where it is possible to excite surface **52**
Figure II 11 Recycling performance of the PR inverse opal (a) Mass recycling efficiency. (b) Stop band position cycling. 0 and 1 represented the status of the PR inverse opal before and after oil sorption, respectively..... **54**

Figure. III. 1 Typical scheme of the gas detection system based on photonic crystals **59**
Figure. III. 3(a) Array layout generation, (b) network presentation **62**
Figure. III. 2 (a) Index profile, (b) Scheme illustrates the geometric parameters of a 2D photon crystal **62**
Figure. III. 4(a) Global Arrangements, (b) Symbol Publisher Table**. 63**
Figure. III. 5 photonic band diagram of the host structure **63**
Figure. III. 6 Transmission spectra of the host stucture for TM polarisation**. 64**

Figure. III. 7 (a) PhC waveguide design formed by omitting a line of air holes. (b) the transmission spectra..... **65**
Figure. III. 8 (a) The proposed design of toxic gas sensor. (b) Schematic illustration of the geometric parameters of the central cavity. (c) Coupled-cavity systems for the realization of resonant effect..... **65**
Figure. III. 9(a)Transmission spectra of the coupled system, (b, c) The 3D distributions of magnetic fields (|H| at different resonant wavelength (Mode 1 and 2), (d) The 2D distributions of magnetic fields (|H| of the second Mode..... **67**
Figure. III. 10 Transmission spectra of sensor varying the refractive index of holes from n = 1 to n = 1.002..... **68**
Figure. III. 11 The variation of the resonant wavelenght (a), transmission (b) and sensitivity (c) as a function of the change of X-Slot. **69**
Figure. III. 12 The variation of the resonant wavelenght (a), transmission (b) and sensitivity (c) as a function of the change of Z-Slot..... **71**
Figure. III. 13optimized sensor..... **72**
Figure. III. 14 The variation of the transmission and sensitivity as a function of the change of RC, (a) Mode 1, (b) Mode 2..... **73**
Figure. III. 15 Transmission spectrum of the optimized Toxic gas sensor, (a) Mode 1, (b) Mode 2 ... **74**

List of Tables:

Table I.1 Optical fiber-based gas sensors..... **15**
Table I.2 Few selective grating-based optical fiberVOCsensors..... **23**
Table III.1 Parameters of the sensors used in this work..... **61**
Table III.2 Range of forbidden bands **64**
Table III. 3 Variation of FWHM**,** Quality factor and FoMasa functionofthechangeofX-Slot **70**
Table III. 4 Variation of FWHM, Quality factor and FoM as a function of the change of Z-Slot **72**

Glossaire :

CP	Cristal Photonique
BP	Bande passante
BIP	Bande Interdite Photonique
BIE	Bande Interdite électromagnétique
BPG	Photonic Band Gap
EBG	Electromagnetic Band Gap
TM	Traverse Magnetic
TE	Traverse electric
1D	Unidimensionnel
2D	Bidimensionnel
VOC	Volatile Organic Compounds
POC	Point-Of-Care
IEQ	The Indoor Environmental Quality
$\boldsymbol{E}$	Electric field (volts/m)
$\boldsymbol{D}$	Electric flux density (coulombs/m^2)
$\boldsymbol{H}$	Magnetic field (amperes/m)
$\boldsymbol{B}$	Magnetic flux density (webers/m)
$\boldsymbol{M}$	Magnetic current density (volts/m^2)
$\boldsymbol{J}$	Electric current density (amperes/m^2)

Nomenclature

λ	Longueur d'onde
$\lambda 0$	Longueur d'onde de résonance
$\lambda cutoff$	Longueur d'onde de coupure
n	Indice de réfraction.
a	Période du cristal photonique
r	Rayon des trous
$neff$	Indice de réfraction effectif.
$S\omega$	La pulsation s sensibility

General introduction

Optical nano-sensors are tiny devices designed to detect and measure environmental factors at an incredibly small scale. These sensors utilize light and nanotechnology to monitor parameters like pollution levels, chemical compositions, and biological contaminants in the environment. Their compact size and high sensitivity enable precise and real-time monitoring, offering valuable insights into environmental health. Optical nano-sensors hold immense potential for revolutionizing environmental monitoring efforts, aiding in the protection and preservation of ecosystems worldwide.

Photonic crystal sensors offer high sensitivity and rapid response for environmental monitoring applications. These sensors detect minute changes in environmental parameters such as air and water quality, pollutant concentrations, and greenhouse gas levels. Their compact design and potential for remote operation make them ideal for creating efficient monitoring networks, providing real-time data crucial for environmental management and decision-making. With their advanced capabilities, photonic crystal sensors are poised to revolutionize how we monitor and protect our environment.

Two-dimensional photonic band gaps (PBGs) refer to ranges of wavelengths in which electromagnetic waves, particularly light, are forbidden from propagating in certain directions within a two-dimensional periodic structure. These structures, often composed of materials with alternating high and low refractive indices arranged in a lattice pattern, create band gaps due to constructive and destructive interference of light waves. PBGs play a crucial role in photonic crystal devices by controlling the flow of light, enabling the manipulation of photons for various applications such as optical communication, sensing, and integrated photonics.

The work of this master thesis is part of this perspective while exploiting a new approach that allows the design and study of refraction index (RI) sensors based on two-dimensional CPs operating in the mid-infrared region. The structures proposed in this work are essentially based on a slotted waveguide-cavity coupling system. We have set ourselves the goal of strengthening the confinement of light within the cavity. In the present work, an ultra-compact 2D-PhC two-dimensional mid-infrared (mid-IR) photonic crystal sensor using slotted-waveguide coupled-cavity for environmental monitoring is designed, and good sensing characteristics such as sensitivity, Q-factor, FOM, detection limit, resonant wavelength, and normalized transmission are estimated for the proposed biosensor. The proposed high-performance PhC mid-IR sensor has a simple structure, an ultra-compact size, and high confinement of light within the

microcavity region. All the simulations are done using Plane Wave Expansion (PWE) method and Finite- Difference Time-Domain (FDTD) tool of RSoft Photonic Suite CAD. To present most of our work, we will give the master thesis the following structure:

The first chapter explores optical nano-sensors' fundamental applications, highlighting their potential to revolutionize environmental safeguarding efforts, since these sensors are characterized by high sensitivity and the ability to detect environmental hazards early.

Then, the second chapter is devoted to an introduction to photonic crystals. We will begin by introducing photonic crystals and presenting their general notions. After a brief recall of the different types of photon crystals, we will focus our study on two-dimensional photon crystals (2D-PhC). This chapter focuses on the study of RI biosensors based on photonic crystals.

Finally, in the last chapter, a slotted waveguide-cavity coupling based on PhCs that can be used for (RI) detection, where the detection of an analytic can be performed by changing (RI) will be designed. We will also study the effect of physical and geometric parameters on the performance of the proposed sensors in order to improve their performance. All simulations will be performed using both the (PWE) and (FDTD) methods of the FullWAVE and BandSOLVE simulator from RSoft Photonic Suite CAD. We will conclude this master thesis with a general conclusion summarizing the results achieved, thus proposing some perspectives.

Chapter I: Optical Nano-Sensor for Environmental Monitoring: Fundamental Application

I.1 Introduction

In the realm of environmental science, the advent of nanotechnology has ushered in a new era of detection and monitoring capabilities. Among these advancements, optical nano-sensors have emerged as a powerful tool for environmental monitoring. These sensors, which operate on the nanoscale, leverage the unique optical properties of nanomaterials to detect and quantify various environmental contaminants with unprecedented sensitivity and specificity. This technology has found fundamental applications in areas such as air, water, and soil quality monitoring, detection of specific contaminants like pesticides, heavy metals, and pathogens, and overall environmental protection. As we continue to face global environmental challenges, the role of optical nano-sensors in environmental monitoring is becoming increasingly crucial. This chapter will delve into the fundamental applications of optical nano-sensors in environmental monitoring, highlighting their potential to revolutionize our approach to safeguarding our planet.

I.2 Optical sensor technology

I.2.1 Nanostructure-Based Sensors

Nanomaterials have been extensively studied for application in various kinds of nanoscale functional devices used widely in the chemical industry, medical diagnostics, food technology, ultra-violet testing, national defense and our daily life. Among these, the semiconductor nanomaterials such as ZnO, SnO_2, TiO_2, and ZnS receive most attention due to intriguing nanosize effects on their physical and chemical properties [1].

I.2.2 Optical Chemical Sensors

Optical sensors, or opt(r)odes, represent a group of chemical sensors in which electromagnetic (EM) radiation is used to generate the analytical signal in a transduction element. The interaction of this radiation with the sample is evaluated from the change of a particular optical parameter and is related to the concentration of the analyte (Blum, 1997). Typically, an optical chemical sensor consists of a chemical recognition phase (sensing element or receptor) coupled with a transduction element (Figure I.1). The receptor identifies a parameter, e.g., the concentration of a given compound, pH, etc., and provides an optical signal proportional to the magnitude of this parameter. The function of the receptor is fulfilled in many cases by a thin layer that can interact with the analyte molecules, catalyse a reaction selectively, or participate in a chemical equilibrium together with the analyte. The transducer translates the

optical signal produced by the receptor into a measurable signal that is suitable for processing by amplification, filtering, recording, and display.

Optical chemical sensors have numerous advantages over conventional electricity-based sensors, such as selectivity, immunity to electromagnetic interference, and safety while working with flammable and explosive compounds. They are also sensitive, inexpensive, non-destructive, and havemany capabilities. Optrodes do not require a reference cell, as isthe case in potentiometry. Furthermore, they can easily be miniaturized and allow multipleanalyses with a single control instrument at a central site [2].

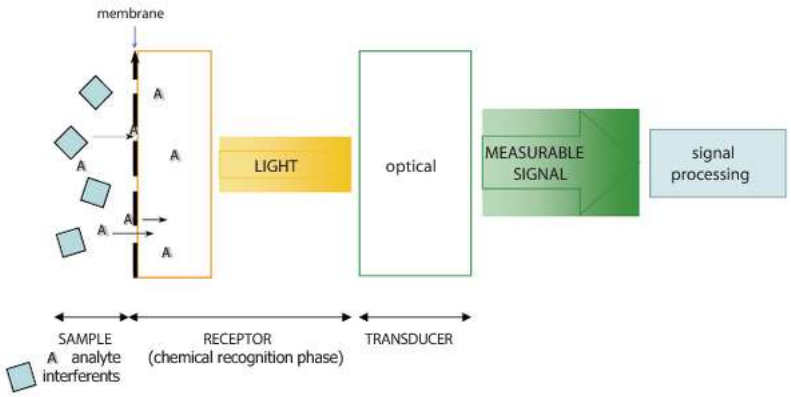

Figure. I. 1Schematic representation of the composition and function of an optical chemical sensor [2].

I.2.3 Photonic Crystal Fiber Sensors

Photonic crystal fiber is a novel type of optical fiber, which acquires its waveguide properties from a photonic crystal structure running along the fiber length. A photonic crystal is a periodic dielectric medium with low losses that is made from a repetitive array of microscopic air holes forming a microstructure. The photonic crystal acts as a cladding for guiding the light, whereas the fiber core may be solid or hollow. The properties of these fibers can be altered by modifying the design of crystal structure and/or by filling air core with gas or liquid which itself is a biggest advantage. Other major advantages of these fibers include efficient light guiding, single-mode operation over an enhanced wavelength range, small nonlinearities, dispersion controlling, and polarization maintenance. The present applications of these fibers include telecom components, sensors, high-power lasers, amplifiers, and medicine[3].

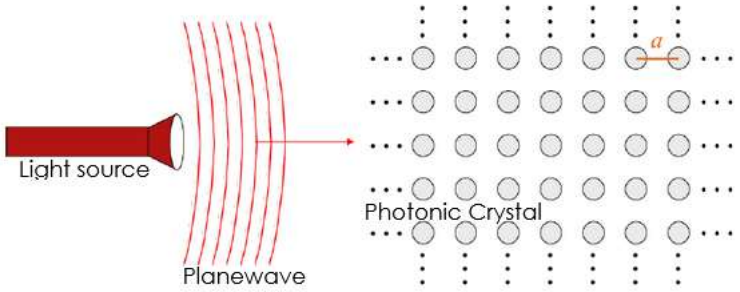

Figure. I. 2A photonic crystal structure interacting with light [3].

I.2.4 Optical biosensors

Opticalbiosensorsrepresentthemostcommontypeofbiosensor.The optical biosensors allow the sensitive and selective,detection of a wide range of analytes including viruses, toxins, drugs, antibodies, tumourbiomarkers and tumour cells.

Optical biosensors offer great advantages over conventional analytical techniques because they enable the direct, real-time and label-free detection of many biological and chemical substances. Their advan- tages include high specificity, sensitivity, small size and cost-effectiveness. Multiple advanced concepts and highly multidisciplinary approaches including microelectronics, microelectromechanical systems (MEMSs), micro/nano-technologies, molecular biology, biotechnology and chemistry are applied in the implementation of new optical biosensors. The research and technological development of optical biosen- sors has experienced an exponential growth over the last decade. Optical biosensor research and devel- opment has been directed mainly towards healthcare, environmental applications and the biotechnology industry. The potential applications of biosensors in the fields of medicine, the environment and biotech - nology are numerous, and each has its own requirements in terms of the concentration of analyte to be measured, the required precision of output, the sample concentration required, the time taken to complete the probe, the time necessary to enable reuse of the biosensor and the cleaning requirements of the system[4].

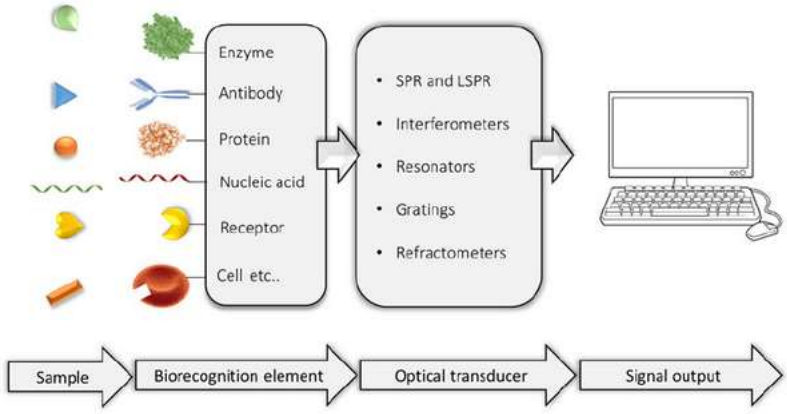

Figure. I. 3 Schematic representation of the Optical biosensors [4].

I.2.5 Optical fiber-based gas sensors

Over the past few decades, Photonic Crystal Fiber (PCF) has made significant progress in the field of optical sensing. Optical fibers now extend beyond telecommunications applications, thanks to advancements in opticalinstrumentation.The PCF, sometimes referred to as holey fiber, consists of infinitesimally small air holes arranged periodically and extending the entire length of the fiber. The typical PCF is composed of fused silica, which has a symmetrical pattern of air holes or voids that operate perpendicularly to its axis. Unlike traditional optical fibers, this fiber has a single material that serves as both the core and the cladding. The development of optical devices and sensors has paid significant attention to PCFs due to their distinctive features, including design flexibility, the ability to regulate light, faster detection speed, and a structure that can be downsized.Additionally, by adjusting the structural characteristics of PCFs, such as the size of the air holes, the pitch, and the number of rings, the evanescent field can be regulated, opening up a wide range of potential applications, especially in sensing. Given that it offers a wide range of uses, including filters [5], switches [6,7], electro-optical modulators [8], polarization converters [9], and sensors [10,11].Recently, Photonic Crystal Fibers (PCF) have garnered significant interest. For several decades, PCF has been extensively explored as a potential candidate for optical sensing. To address safety concerns, highly sensitive liquid and gas sensors are essential in industrial operations, especially for detecting poisonous and flammable gases or liquids. Therefore, improving the performance of liquid and gas sensors has emerged as a serious issue. Liquid and gas detection based on Photonic Crystal Fibers have shown reliable results in terms of sensitivity and responsiveness. Recently, researchers have shown a lot of interest in developing a PCF-based system for environmental

and public safety detection [12-13].In the field of environmental monitoring, a Mach-Zehnder Interferometer (MZI) based on a Hollow Core Photonic Crystal Fiber (HC-PCF) is introduced. This device, as depicted in Figure.I.4a [14], can detect ambient CO_2 levels. The device was created by sandwiching a stub of HC-PCF between a lead-in and lead-out Single Mode Fiber (SMF).The sensor was calibrated for specific CO_2 gas concentrations and demonstrated a linear response to CO_2 levels with a sensitivity of 4.3 pm/% CO_2 at atmospheric pressure and room temperature. The precision of the sensor is 0.2% CO_2, considering that the measuring tool used in this study has a wavelength stability of 1 pm. The sensor showed rapid reaction and recovery times of 64 and 69 seconds, respectively, for a test chamber dimension of 14.5×11.2×4.4 cm. The sensor was enclosed in gas-permeable, water-resistant membranes. This sensing device demonstrated the ability to monitor CO_2 levels in both underground and aquatic conditions and detect laboratory-level leaks. The sensor consistently and accurately detected CO_2 concentrations, exhibiting remarkably quick reaction and recovery times. The schematic presented in Figure.I.4b is used to characterize CO_2 gas concentration in near atmospheric pressure [14]. According to the experimental research of this work [14], fiber-optic technology shows promise for monitoring CO_2 content and leakage in the environment. A Fiber Bragg Grating (FBG) was also inserted in the chamber to monitor any temperature changes that occurred throughout the tests.Figure 3c illustrates how the sensor exhibits a regular pattern of changes in response to varying CO_2 gas concentrations. Figure 4d depicts the sensor's reaction to a change in room temperature between 25°C and 65°C. The sensor exhibits a uniform spectral shift with temperature change with a sensitivity of 31.67 pm/°C [14]. the sensorexhibits a uniform spectral shift with temperature change [14]. A few important works on optical fiber-based gas sensors are presented in Table I.1.

Material for Selective Sensing	Gas Detection	Sensitivity	LOD (%)	Range (%)
Crytophane E	Methane	−1.6 nm/%	0.06	0–5
Graphene + Ag	Methane	0.34 nm/%	0.1	0–3.5
Crytophane A	Methane	6.39 nm/%	0.015	0–3.5
Carbon nanotubes	Carbon dioxide	0.04 nm/%	0.05	0–100
Nickel oxide and reduced graphene oxide	Carbon dioxide	1400 a.u/%	0.0005	0–0.05
Carbon nanotubes and polyallylamine	Carbon dioxide	0.1 nm/%	0.01	0.1–0.4
Divinylbenzne and siloxane polymer	Nitrous oxides	5×10^7 dB/%	10^7	$0–1.8 \times 10^{-6}$
Carbon nanotubes, polyethyleneimine, Au	Nitrous oxides	0.05 nm/%	0.0109	0–100
	Nitrous oxides	82 μV/%	0.001	0–2.5
Graphene oxide	Water vapor	0.349 dB/%	0.2	30–77
Chitosan	Water vapor	0.107 nm/%	0.1	30–77
Graphene quantum dots	Water vapor	0.567 nm/%	0.05	11–85

Table I. 1 Optical fiber-based gas sensors

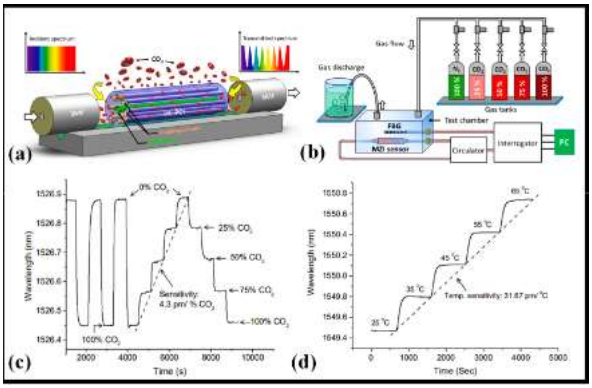

Figure. I. 4HC-PCF-based gas sensor, (a) schematic of MZI developed using a small stub of HC-PCF, (b) experimental schematic for sensor characterization and interrogation, (c) the response of thesensor to CO2 gas concentration, (d) the response of the sensor to time

I.2.6 Optical waveguide-based gas sensors

The mid-infrared (mid-IR) spectral region has recently garnered significant interest, as it holds the potential to realize several intriguing possibilities [15-16]. This is due to the presence of absorption peaks of many trace gases, including CO, CO_2, NO, NH_3, and CH_4, among others [17-18]. These gases experience significant absorption in the mid-IR region > 2.5 µm due to fundamental rotational and vibrational transitions. Recently, several gas sensors have been developedA variety of sensor systems have been introduced based on different technologies and platforms, including electrochemical sensors [19], spectroscopic approach [20], and gas chromatography [21], among others. Most of these sensor systems are large in size and typically expensive, making them impractical or not user-friendly. The fundamental building block of a wide range of optical sensors is a nanophotonic waveguide [22]. In this context, optical waveguides built on the SOI platform provide an attractive alternative that uses evanescent field absorption sensing to detect trace gases. Evanescent field absorption-based gas sensors are only effective when the gas being measured exhibits a characteristic absorption line at the relevant wavelength.

Additionally,there is a correlation between the optical attenuation at a certain wavelength and the gas content. Numerous gas sensors based on optical waveguides [23-24] and optical fiber [25-26] have been developed to operate on this phenomenon.

Recently, there has been a spike in demand for gas detectors that are miniaturized and CMOS compatible. Optical techniques may be quicker and more reliable than sensors that use metal-oxide chemical interactions. A combination of an external laser source and silicon

waveguides built using CMOS technology has lately been used to perform CO_2 detection by evanescent-wave absorption in the mid-infrared [27]. In [22], it is shown that a low-cost integrated heat source can detect CO, at concentrations as low as 3%. A schematic of the proposed gas sensor and measuring setup is shown in Figure I. 4a [22]. A compact gas container (Figure I. 5b) containing the sensor chip is continually flushed with a combination of CO_2 and N_2 gas. Two openings on the top of the chamber serve as the departure points for the gas and are designed to receive the optical fiber and electrical connections. A mass-flow control device regulates the concentration of the two gases in the mixture, and the gas moves at a rate of 100 ml./min. By lowering the flow speed to lesser values, no difference in the measured transmittance was seen. New designs are now being developed to raise the still relatively low sensitivity since these results are encouraging for future technical advancements toward on-chip mid-infrared photonic gas sensors.It is suggested to use a hybrid plasmonic waveguide (HPWG) with a polarization- insensitive design that is tuned to the methane gas absorption line at 3.392 µm wave length [28]. The schematic of the waveguide is shown in Figure I.5c. For both transverse electric (TE) and transverse magnetic (TM) hybrid modes, the waveguide design can offer high mode sensitivity (Smode) and evanescent field ratio (EFR) Sende and EFR of 0.94 and 0.704, respectively,can be produced for the TE hybrid mode at optimum waveguide specifications, whereas Smate and EFR of 0.86 and 0.67, respectively, can be obtained for the TM hybrid mode. At a 60% gas concentration, a 20 um-long HPWG can dissipate power in the TE and TM hybrid modes by around 3 dB [28],On photonic devices, waveguide structures limit light along predetermined routes and enable interaction between light and matter through an evanescent field [29]. For sensitive applications such as trace gas detection, waveguides still fall short of free space optics. On-chip gas sensing is still in its infancy due, among other things, short optical pathlengths, weak interactions, and erroneous etalon fringes in spectrum transmission Reference [30] describes a mid-infrared integrated waveguide sensor that satisfactorily overcomes these issues. In terms of the optical interaction per length, this sensor works with an evanescent field confinement factor of 107% in air, which not only complements but substantially beats free-space beams. The SEM image of the suspended rib waveguide is shown in Figure I.5d [30]. With only a 2 cm long waveguide, the sensor's performance at 2.566 µm demonstrated a 7 ppm detection limit for a cetylene

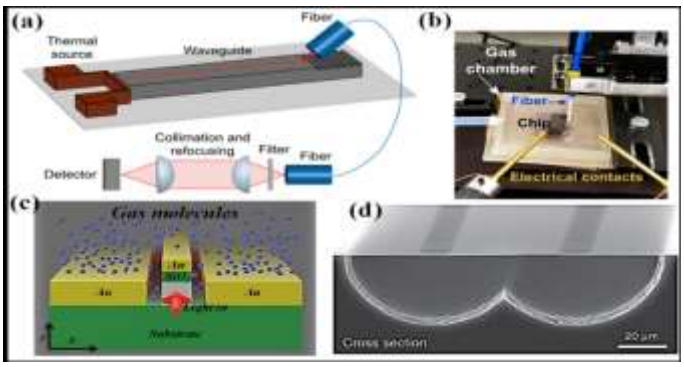

Figure. I. 5Recently proposed waveguide-based gas sensors, (a) schematic view of the gas sensor measuring setup [22], (b) experimental realization of the gas cell [22], (c) schematic of the polarization independent hybrid plasmonic waveguide for gas sensing [28].

I.3 Types of Environmental Monitoring Optical Sensors

In this section, recent developments in the field of optical sensing devices related to four vital environmental parameters are being discussed.

I.3.1 Toxic gas monitoring sensors

Due to environmental and safety considerations, there is now a growing interest in developing optical gas sensor devices [31-32]. Compared to traditional sensors, optical fiber systems have advantages that include inherent safety due to their non-electrical nature, the ability to remotely access hazardous locations, and the potential to support distributed or quasi-distributed systems.Unfortunately, the fundamental characteristics of gas absorption are often in the infrared (IR) region, which falls outside the transmission window of silica fibers. However, there are several related gases that also feature additional and composite absorption lines in the near-infrared region (1=1–2 micrometers), which can be detected using silica fibers and LED or laser light sources [33-34].Examples of these gases include methane (CH_4), carbon monoxide (CO), carbon dioxide (CO_2), and hydrogen sulfide (H_2S). Future developments in mid-infrared sources, fibers, and detection devices will be crucial, as these lines are often 200 times weaker than the fundamental absorption characteristics.

I.3.2 Water quality monitoring sensors

Water, which is one of the most essential natural resources for human life and fundamental for activities such as climate regulation, becomes polluted when contaminants are added to water sources like aquifers, lakes, rivers, seas, and groundwater. The reason for most

of the garbage and pollutants that end up in water bodies each year is due to human activity associated with industrial, touristic, and urban operations. Domestic garbage, waste from food processing, volatile organic compounds, heavy metals, pesticides, pollutants from livestock operations, and chemical waste are just some examples of the diverse pollutantsthat end up in waterways. The chemical composition of aquatic ecosystems and biodiversity continuously deteriorate due to the outflow of these toxins and theheavy use of water resources. Pathogens, which are mostly associated with residential wastewater and cause diseases that are transmitted through polluted water, are another significant category of pollutants. In addition, the spread of pollutants to people and the rest of the biota often occurs through water. Examples include nutrient pollution, which promotes the growth of toxic algae that harm other aquatic species, and pesticides that interfere with plant photosynthesis[35].

I.3.3 Indoor environment monitoring

The Indoor Environmental Quality (IEQ) refers to the set of conditions inside a building and how they affect its inhabitants. These conditions include air quality, lighting, temperature, and environmental factors. When IEQ is improved, the commercial value of the building increases and the quality of life, health, and productivity of its inhabitants improve. The main goal of IEQ is to reduce the risk of health problems during work and to provide a comfortable and conducive environment for productivity for those who work there. Given the ongoing impact of the global pandemic, it is clear that this program is now more important than it was before[36].

I.3.4 Natural disaster monitoring

Natural disasters are catastrophic events resulting from the planet's natural processes, including earthquakes, tsunamis, floods, and storms. Throughout the Earth's existence, estimated at about 4.5 billion years, the Earth has witnessed numerous natural disasters. Some of these disasters have led to mass extinctions and significant impacts on the remaining species [37]. In addition, some natural threats may be caused by or influenced by human activities [38]. Diverse activities such as mining, agriculture, and deforestation can cause landslides [39]. Natural disasters can cause extensive damage, as they can destroy animal habitats, such as wildfires, which can also cause property damage and fatalities.

I.4 Environmental monitoring applications

I.4.1 Volatile organic compounds monitoring

Volatile organic compounds (VOCs) are always present in nature and are crucial for plant-to-plant and plant-to-animals interactions. While most VOCs derived from natural and biological sources do not provide health or environmental risks, this is not the case for VOCs derived from human sources. VOCs produced by humans are typically linked to pollution, respiratory illnesses, and harm to vital organs and systems such as the liver, kidneys, and central nervous system. VOCs do represent a health concern, with some of them being very poisonous or causing long-term harm. Tracking the concentrations of VOCs in indoor and outdoor air as well as water systems is becoming more important in the present climate of escalating environmental and health concerns. Conventional techniques for detecting VOCs rely on mass spectrometry [40], gas chromatography [41] and high-performance liquid chromatography methods [42]. The practical distribution and implementation of these approaches for real-time water or air quality surveillance are hindered by their expense, time commitment, and bulkiness irrespective of the fact that they are precise and selective. Utilization of MEMS sensors [43] and MOS transistor-based sensors [44], which are based on the electrical resistance or resonant frequency shift when VOCs adsorb on the surface of a metal oxide or piezoelectric film, respectively, are other relatively common VOC detection methods. These sensors solve issues such as test expense, bulky equipment, and lengthy processing times in the laboratory of traditional approaches. However, their high operating temperatures between 200 and 400°C- require the use of a heater for on-chip temperature regulation, negating the benefits of both MOS and MEMS technologies' low-power operation. Additionally, selectivity to certain compounds is constrained [45-47].

A proposal is made for a VOC sensor architecture that addresses typical issues with photonic integrated sensors, such as reusability and specificity [48]. The suggested sensor includes chemically selective polydimethylsiloxane (PDMS) polymer cladding that encloses the waveguides and offers an extensible and permeable low-refractive index material. It is based on arrayed waveguide interference and is constructed on an SOI platform. In the context of environmental and public health protection, it is crucial to monitor the occurrence of certain volatile organic chemicals, which this cladding material serves as the chemical transducer element by altering its optical characteristics when in contact. The sensor works at room temperature, and several experiments using water, toluene, chlorobenzene, and hexane validated its selectivity. These tests also established the sensor's durability. At a central

wavelength of 1566.7 nm, verification with chlorobenzene resulted in a maximum spectral shift of around 22.8 nm. Additionally, at mass percent concentrations of chlorobenzene, a sensitivity of 234.8 pm/% was found, with a limit of detection of 0.24% m/m. The sensor's thermal sensitivity was determined to be 0.9 nm/°C [48].

To investigate VOCs, silicon nitride (SiN) waveguide-based mid-IR sensors were developed and tested [49]. With a lower refractive index than common materials such as Si, SiN thin films made using low-pressure chemical vapor deposition (LPCVD) have a wider mid-IR transparent zone, which results in a stronger evanescent wave and increased sensitivity. Additionally, experimental proof of in situ monitoring of three VOCs (acetone, ethanol, and isoprene) was provided by measurements of their distinctive absorption at wavelengths between 3.0 and 3.6 µm. Due to its greater evanescent field than the Si waveguide, the SiN waveguide demonstrated a five-fold gain in sensitivity. As a result, the devised waveguide sensor has the prospective to be employed as a small device module that can monitor a variety of gaseous analytes for purposes in the areas of agriculture, environmental monitoring, and health monitoring.

VOC detection is a subject of considerable interest with applications in many industries, including the food and chemical industries as well as environmental usage [50]. Over twenty years ago, optical fiber VOC sensors with novel and intriguing features that addressed some of the drawbacks of conventional gas sensors were introduced [51]. These sensors are a promising substitute for electronic ones in electrically noisy environments where electronic sensors cannot function properly because of their minimally invasive nature and the benefits that optical fiber provides, such as lightweight, passive nature, low attenuation, and the potential for multiplexing, among others [52]. There are certain evanescent wave sensor designs that do not employ a chemical dye [53]. For instance, it is possible to manufacture the cladding so that it is sensitive to particular organic va- pors; another option is to taper the fiber, which results in a more delicate but sensitive sensor [54-56], or even use an optical fiber without a cladding so that the organic vapors themselves act as a cladding [57].

Most grating sensors that have been created and are now on the market are set up to detect temperature and strain. Meanwhile, Topliss et al. developed a unique VOC sensor design utilizing LPG in 2010 that was based on the wavelength interrogation approach [58]. The LPG fiber has been covered with a coating of calixarene, which demonstrates excellent sensitivity to aromatic chemicals such as benzene and toluene while being somewhat susceptible to other

aliphatic hydrocarbons such as hexane. The monitoring of different VOCs using a unique selective chemical sensing method is described [52]. This method involves depositing PDMS on FBG structures. The sensor was built using awavelength interrogation approach that took the use of the coating of PDMS on FBG's swelling response when VOCs are present. The FBG receives a tensile tensionfrom the swelling action. The swelling ratio of the sensing material has a significant impact on how much of this tensiletension is applied to the fiber. Therefore, by examining the Bragg wavelength shift of the PDMS-deposited FBG, the type and concentration of exposed VOCs may be precisely and selectively detected. Fig I.6a displays the reported sensor's schematic representation [52]. The sensor was evaluated using acetone, methanol, 1- and 2-propanol. A redshift in the resonance wavelength associated with each VOC is seen in Fig I.6b [52]. The use of LPG coated with the novel sensing substance silk fibroin to create a VOC sensor for methanol detection is disclosed [59]. A thin layer of silk fibroin sensing film that was created on LPG using the drop-casting process makes up the sensor. Based on a wavelength interrogation approach, the sensor was used. As part of the setup, a sensitive manometer was installed in the gas chamber to monitor pressure changes brought on by the evaporation of the methanol that was supplied liquidly through the input. For methanol fluctuating between 80 and 100 mbar, the disclosed sensor shows a high sensitivity of 0.22 nm/mbar. This was the first time the function of the fibroin protein in the detection of VOCs with a good reversible response had been investigated [59]. Table I.2 presents a few selective optical fiber grating-based VOC sensors recently proposed.

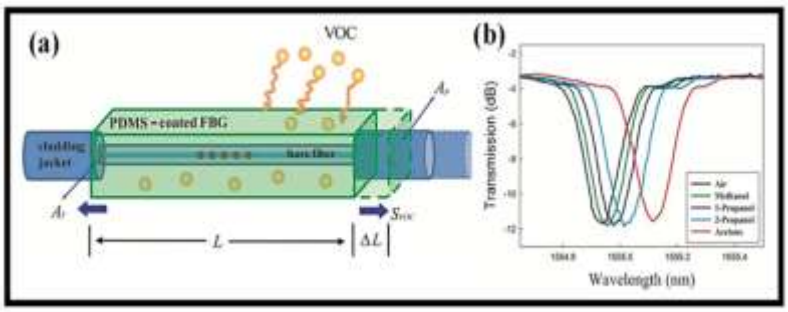

Figure. I. 6(a) PDMS-coated FBG sensor schematic diagram [52], (b) sensor spectral response for each VOC [52].

Grating Type	Sensing Material	Target VOC	Sensitivity	Operating Range
LPG	Zeolite imidazolate framework	Ethanol, acetone, and methanol	0.015 ± 0.001 nm/RIU for acetone and 0.018 ± 0.0015 nm/ppm for ethanol	987–19,700 ppm for acetone 1240 to 24,800 ppm for ethanol
LPG	PDMS	Xylene and cyclohexane	19 nm/50% for xylene	-
FBG	Diphenilalanine nanotubes	Methanol	(−7.3 ± 0.8) pm/(%o/o)	-
LPG	ZnO nanorod	Ethanol	Measure in refractive index variation	100 min exposure time
FBG	PMMA	Ethanol	Linear response for 3% concentration	-
D-shape FBG	PDMS	Dichloromethane, Acetone	4000 ppm, 6000 ppm	0–90,000 ppm
TFBG	Molecularly imprinted polymer	Ethanol, acetone, toluene	0.44 pm/ppm, 0.38 pm/ppm, 0.28 pm/ppm	0–17 ppm
LPG	PDMS	Acetone	9.4×10^{-4} ppm^{-1}	-
4 FBG	Hydrophobic siloxane co-polymer	Hydrocarbons	-	-

Table I. 2 Few selective grating-based optical fiber VOC sensors

I.4.2 Organ-phosphorus compounds monitoring

Organ phosphorus compounds are the most important of environmental pollutants. organ phosphorus compounds are stable in water and temperature relatively. The environmental effects of organ phosphorus compounds are clear for all people. Some of them are destructive and fatal so that, their production, uses, storage, development and destruction are under control of international organizations such as UN and EPA. Many techniques are suggested for extraction organ phosphorus compounds in water. In this research work, the liquid – liquid extraction (LLE) and liquid – liquid micro extraction was used for extraction of organ phosphorus compounds. GC/MS-Ion trap system with two ionization sources (El and Cl) was used for separation and identification of mentioned compounds. Selected Ion Monitoring (SIM) technique was used for more confirmation too. Three locations in the Anzali lagoon water were selected for sampling and after chemical treatments and analysis many organ phosphorus compounds were detected and identified by ion trap system[60].

I.4.3 Heavy metal ions monitoring

An increase in heavy metal ions (HMIs) in the environment has numerous harmful effects on the environment, human health, and other organisms. In recent years, this problem has raised serious concerns as a result of industrialization and has led to the development of devices to detect and monitor HMI devices in the environment. Although there are different analytical tools being used, they are expensive, tedious, difficult to handle, bulky and not portable. These issues have been addressed in the development of point-of-care testing (POCT) devices that are economical, portable, and easier to handle. These devices also provide the

advantages of on-site monitoring of HMI devices, a task that is difficult to perform with conventional devices and this has helped in the development of point-of-care testing in recent years. Therefore, this review includes recent advances in on-site HMI monitoring using point-of-care testing devices based on colorimetric, fluorometric, and electrochemical techniques[61].

I.4.4 Endocrine disrupting chemicals monitoring

Endocrine disrupting chemicals (EDCs) are harmful, xenobiotic compounds requiring a multi-tiered analytical approach for a reliable management. Although worth efforts worldwide, comprehensive EDCs monitoring and risk-assessment still require improvements.

Risks for public health due to EDCs exposure, and revises the maturity reached in different analytical detection fields, with a special focus on biosensor technology. Among validated laboratory-techniques, hyphenated mass-spectrometry-based chromatography provides high selectivity and multi-analyte detection, while in vitro bioassays enable reliable toxicological testing. However, none of these methods is suitable for fast in field, continuous or semi-continuous operations. Due to advances in material science and synthetic biology, now biosensor technology holds the promise to close this gap and, although not included yet in routinely screening programs, fulfill the necessary requirements to sustain a coherent and global strategy to assess the state of environmental pollution [62].

I.5 Photonic crystal chemical sensors for environmental monitoring

I.5.1 Definition

The nanostructured materials such as nanoparticles have great possibilities as a novel sensing device. In this study, development of the photonic crystal based optical chemical sensor for environmental monitoring was aimed. The sensor consists of a glass substrate with a three-dimensional photonic crystal using nanoparticles and poly(dimethylsiloxane) (PDMS) elastomer. Such a photonic crystal was generated by infiltrating the voids within an opaline lattice of nanoparticles with a liquid prepolymer to PDMS, followed by thermal curing. When a nonpolar organic solvent capable of swelling the elastomer matrix, was introduced to the surface of this sensor, the lattice constant and thus the wavelength of Bragg diffracted light was increased. On the basis of this mechanism, we demonstrated the detection of volatile organic compounds (VOCs). As a result, this photonic crystal based optical chemical sensor could be used to specifically determine the VOCs concentrations. Additionally, using this photonic crystal based optical chemical sensor, the change in the optical characteristics could be observed

with the naked eye. Therefore, this optical chemical sensor can be applicable to on-site monitoring for environmental application[63].

I.5.2 Fabrication of the photonic crystal based opticalchemical sensor

In this experiments, polystyrene (PS) nanoparticles (particle diameter: 202 nm) were used to form the photonic crystals. The first step involved the fabrication of photonic crystals by drying aqueous dispersions of PS nanoparticles on the glass substrates. In this experiment, 20 µl of the polystyrene nanoparticle dispersion (2.0% w/v) was introduced on the surface of a slide glass substrate to form a thin layer of liquid film. Finally, this sample was placed under ambient laboratory conditions to allow the water to evaporate. The PS nanoparticles were driven into a long-range ordered, opaline lattice by the attractive capillary forces generated during water evaporation. After the dry-up process of the nanoparticle dispersion, the PDMS solution (50 µl) was then distributed on the top of the photonic crystal, and the voids between the PS nanoparticles were completely filled with the premixed elastomer of PDMS through capillary action. The elastomer was then cured at room temperature overnight, followed by additional baking at 60 °C for 1 h. In this study, in order to fabricate of the photonic crystal based optical chemical sensor using PDMS, a curing agent and the PDMS prepolymer were mixed in a 1:10 ratio by weight. The PDMS solution was degassed in desiccators with a mechanical vacuum pump to remove any air bubbles in the solution and ensure complete mixing between the two parts. Thus, these fabrication procedures resulted in the fabrication of a photonic crystal based optical chemical sensor[64].

I.5.3 Surface analysis of the photonic crystal using atomic force microscopy

To analyze the surface quality of the photonic crystal in terms of particle density and periodicity, atomic force microscopy (AFM) was carried out in tapping mode using silicon tips and cantilevers with a nominal spring constant of 13 N/m for scanning in air. All reported images were acquired at scan rates in the range 0.25-0.50 Hz[64].

I.5.4 Colorimetric detection of BTX using the photonic crystalbased optical chemical sensor

To evaluate the optical characteristics of the photonic crystal based optical chemical sensor, all absorbance spectra were taken from 400 to 800 nm on the UV-VIS spectrometer at RT. Under these experimental conditions, the optical characteristics of the photonic crystal based optical chemical sensor were investigated. In addition, to evaluate the sensing capability of this sensor, different kinds of organic solvents (ethanol, methanol, 2-propanol, acetone,

benzene, toluene, and xylene) and ultra pure water were introduced onto its surface and its optical characteristics were measured. Simultaneously, we measured the change in its optical characteristics with time (0, 1, 2, 5, and 10 min) due to the swelling of the PDMS and evaluated its calibration characteristics by introducing different concentrations of nonpolar organic solvents[64].

I.5.5 Characteristics of the photonic crystal based opticalchemical sensor

FigI.7 shows the absorbance characteristics of the photonic crystal based optical chemical sensor from visible (violet color) to near-IR wavelengths using several kinds of diameters of nanoparticles. From these characteristics, 202 nm of PS nanoparticles were used for fabrication of photonic ying crystal based optical chemical sensor respectively (Fig I.8a). In addition, the structural color due to Bragg reflection could be observed in visible region (peak wavelength: 552 nm) that fabricated using 202 nm PS nanoparticles (Fig I.8b)[64].

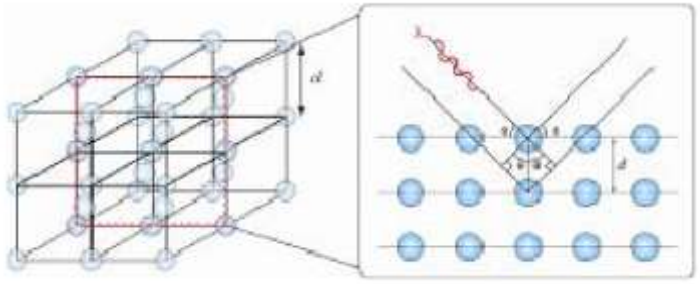

Figure. I. 7Theoretical schematic illustration of the photonic crystal.

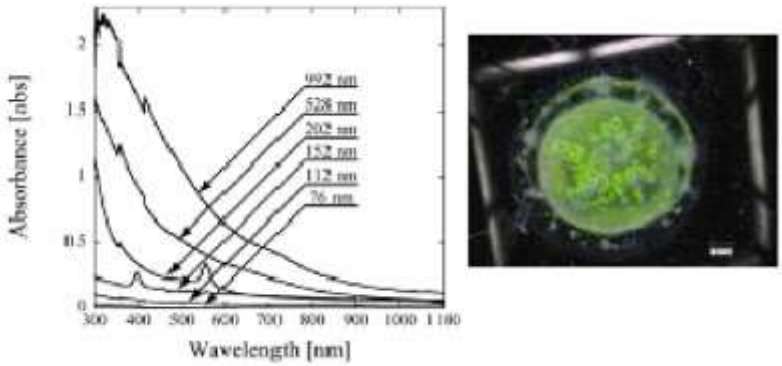

Figure. I. 8Optical characteristics of photonic crystal based optical.

I.5.6 Colorimetric detection of organic solvents using the photonic crystal based optical chemical sensor

The colorimetric detection of different kinds of organic solvents using photonic crystal based optical chemical sensors was carried out. 500 µl of different organic solvents was introduced onto the optical chemical sensor surface, and the changes in its optical characteristics were investigated. FigI.9 shows the changes in the optical characteristics with time of the photonic crystal based optical chemical sensor in the visible region (400~800 nm). When the xylene was introduced onto the optical chemical sensor surfaces, a change in its optical characteristics could be observed[64].

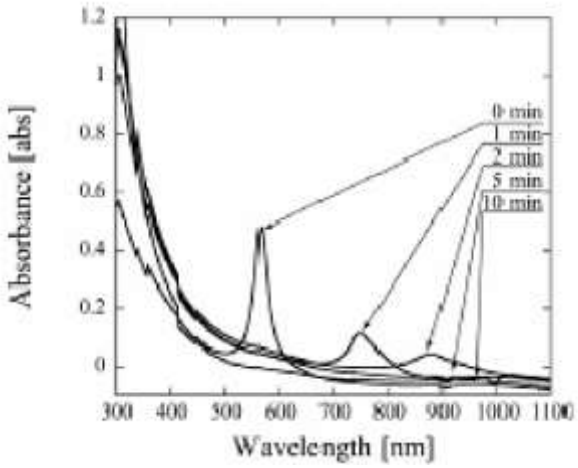

Figure. I. 9Change in the optical characteristics due to the introduction of xylene.

I.6 Conclusion

In conclusion, the application of optical nanosensors in environmental monitoring represents a major step towards a more sustainable and healthier environment. These sensors are characterized by high sensitivity and the ability to detect environmental hazards early. Integration with modern technologies such as the Internet of Things and artificial intelligence opens new horizons for smart environmental management systems. However, it requires addressing challenges such as sensor robustness, data security, and the need for standardization. Ultimately, nanophotonic sensors are a promising tool in addressing complex environmental challenges.

References:

[1] Ang Wei,Liuhua Pan, Wei H Huang,Materials Science and Engineering, 2011,p.1409.

[2]Aleksandra Lobnik,MatejkaTurel,Spela KorentUrek, Advances in Chemical Sensors, 2012,p.3.

[3]Abdul Rauf, Article,Photonic Crystal Fiber,National University of Sciences and Technology,2014,p. 1.

[4] Pavel Damborský,Juraj Švitel,Jaroslav Katrlík,Opticalbiosensors Essays in Biochemistry, 2016.

[5]Wang, G. Li, S. An, G. Wang, X. Zhao, Y. Zhang, W, Design of a polarized filtering photonic-crystal fiber with gold-coated airholes. Appl. Opt. 2015, 54, 8817–8820.

[6]Cui, K. Zhao, Q. Feng, X.Huang, Y. Li, Y.Wang, D. Zhang, W, Thermo-optic switch based on transmission-dip shifting in adouble-slot photonic crystal waveguide,Appl. Phys, Lett,2012, 100, 201102.

[7] Fasihi, K. High-contrast all-optical controllable switching and routine in nonlinear photonic crystals. J. Light. Technol. 2014, 32,3126–3131.

[8]Huang, Y. Wang, Y. Zhang, L.Shao, Y.Zhang, F.Liao, C.Wang, Y. Tunable Electro-Optical Modulator Based on a PhotonicCrystal Fiber Selectively Filled With Liquid Crystal. J. Light. Technol. 2019, 37, 1903–1908

[9]Zhang, Z. Tsuji, Y.Eguchi, M. Chen, C. Design of polarization converter based on photonic crystal fiber with anisotropic lattice core consisting of circular holes. J. Opt. Soc. Am. B 2017, 34, 2227–2232.

[10]Yan, X. Li, B.; Cheng, T. Li, S. Analysis of High Sensitivity Photonic Crystal Fiber Sensor Based on Surface Plasmon Resonance ofRefractive Indexes of Liquids. Sensors 2018, 18, 2922

[11]Singh, S. Kaur, V. Photonic crystal fiber sensor based on sensing ring for different blood components: Design and analysis. InProceedings of the 2017 Ninth International Conference on Ubiquitous and Future Networks (ICUFN), Milan, Italy, 2017, pp. 399–403.

[12]Whitenett, G. Stewart, G. Atherton, K. Culshaw, B.Johnstone, W. Optical fibre instrumentation for environmental monitoringapplications. J. Opt. A Pure Appl. Opt. 2003, 5, p .140–145.

[13]Carvalho, J.P. Lehmann, H. Bartelt, H. Magalhães, F.Amezcua-Correa, R.Santos, J.L. Van Roosbroeck, J.Araújo, F.M.Ferreira, L.A. Knight, J. Remote System for Detection of Low-Levels of Methane Based on Photonic Crystal Fibres and Wavelength Modulation Spectroscopy. J. Sens. 2009, 2009, 398403.

[14]Ahmed, F. Ahsani, V. Nazeri, K. Marzband, E. Bradley, C.Toyserkani, E. Jun, M.B.G. Monitoring of Carbon Dioxide Using Hollow-Core Photonic Crystal Fiber Mach–Zehnder Interferometer. Sensors 2019, 19, 3357.

[15]Ilev, I. Waynant, R. Mid-Infrared Biomedical Applications. In Mid-Infrared Semiconductor Optoelectronics; A. Krier, Ed.; Springer:London, UK, 2006.

[16]Popa, D.Udrea, F. Towards Integrated Mid-Infrared Gas Sensors. Sensors 2019, 19, 2076.

[17]Pal, S.Ozanyan, K.B. McCann, H. A spectroscopic study for detection of carbon-monoxide using mid-infrared techniques for single-pass measurement. J. Phys. Conf. Ser. 2007, 85, 012020.

[18]Siebert, R. Müller, J. Infrared integrated optical evanescent field sensor for gas analysis: Part I: System design. Sens. Actuators A Phys. 2005, 119, 138–149.

[19]Liu, T.Wang, X.; Li, L.Yu, J. Review-electrochemical NOx gas sensors based on stabilized zinconia. J. Electrochem. Soc. 2017, 164, B610–B619.

[20]Avetisov, V. Bjoroey, O. Wang, J.Geiser, P. Paulsen, K.G. Hydrogen Sensor Based on Tunable Diode Laser Absorption Spectroscopy. Sensors 2019, 19, 5313.

[21]Zampolli, S. Elmi, I. Stürmann, J.Nicoletti, S.Dori, L. Cardinali, G. Selectivity enhancement of metal oxide gas sensors using a micromachined gas chromatographic column. Sens. Actuators B Chem. 2005, 105, 400–406.

[22]Consani, C. Ranacher, C. Tortschanoff, A.Grille, T.Irsigler, P. Jakoby, B. Evanescent-Wave Gas Sensing Using an Integrated Thermal Light Source. Multidiscip. Digit. Publ. Inst. Proc. 2017, 1, 550.

[23]Guo, Q. Zhang, J. Yang, K.Zhu, Y. Lu, Q. Zhuo, N. Zhai, S.Liu, J.Wang, L. Liu, S. et al. Monolithically integrated mid-infrared sensor with a millimeter-scale sensing range. Opt. Express. 2022, 30, 40657–40665.

[24]Butt, M. Khonina, S.Kazanskiy, N. Optical elements based on silicon photonics. Comput. Opt. 2019, 43, 1079–1083.

[25]Khijwania, S. Gupta, B. Fiber optic evanescent field absorption sensor: Effect of fiber parameters and geometry of the probe. Opt. Quantum Electron. 1999, 31, 625–636

[26]Gupta, B.D.; Singh, C.D. Fiber-optic evanescent field absorption sensor: A theoretical evaluation. Fiber Integr. Opt. 1994, 13,433–443

[27]Anacher, C.Consani, C.Hedenig, U.; Grille, T. Lavchiev, V. Jakoby, B. A photonic silicon waveguide gas sensor using evanescent-wave absorption. In Proceedings of the 2016 IEEE Sensors, Orlando, FL, USA, 2016; pp. 1–3.

[28]Kazanskiy, N.L. Khonina, S.N.Butt, M.A. Polarization-Insensitive Hybrid Plasmonic Waveguide Design for Evanescent Field Absorption Gas Sensor. Photon-Sensors 2021, 11, 279–290.

[29]Kazanskiy, N.Butt, M. Degtyarev, S. Khonina, S. Achievements in the development of plasmonic waveguide sensors for measuring the refractive index. Comput. Opt. 2020, 44, 295–318.

[30]Vlk, M. Datta, A. Alberti, S. Yallew, H.D. Mittal, V.Murugan, G.S. Jágerská, J. Extraordinary evanescent field confinement waveguide sensor for mid-infrared trace gas spectroscopy. Light Sci. Appl. 2021, 10, 26.

[31] Stewart, G. Jin, W.Culshaw, B. Prospects for fibre-optic evanescent-field gas sensors using absorption in the near-infrared. Sens.Actuators B Chem. 1997, 38, 42–47.

[32]Uehara, K. Tai, H. Remote detection of methane with a 1.66 micron diode laser. Appl. Opt. 1992, 31, 809–81.

[33]Tai, H.Yamamoto, K. Uchida, M.; Osawa, S. Uehara, K. Long distance simultaneous detection of methane and acethylene byusing diode lasers coupled with optical fibres. IEEE Photon. Technol. Lett. 1992, 4, pp. 804–807.

[34]Weldon, V. O'Gorman, J. Phelan, P. Tanbun-Ek, T. Gas sensing with wavelength=1.57 microns distributed feedback laser diodesusing overtone and combination band absorption. Opt. Eng. 1994, 33, pp. 3867–3870.

[35] Butt, M.A. Voronkov, G.S. Grakhova, E.P. Kutluyarov, R.V. Kazanskiy, N.L. Khonina, S.N. Environmental Monitoring: A Comprehensive Review on Optical Waveguide and Fiber-Based Sensors. Biosensors 2022, 12, 1038.

[36] Qi Wu, Nianping Li, Xinran Cai, Yingdong He, Yujiao Du, Impact of indoor environmental quality (IEQ) factors on occupants' environmental perception and satisfaction in hospital wards, Building and Environment, vol: 245, 1, 2023, 110918

[37] Gupta, P. Khanna, A. Majumdar, S. Disaster management in flash floods in Leh (Ladakh): A case study. Indian J. Community Med.2012, 37, 185–190

[38] Magnan, A.K. Pörtner, H.-O. Duvat, V.K.E.Garschagen, M.; Guinder, V.A. Zommers, Z. Hoegh-Guldberg, O. Gattuso, J.-P. Estimating the global risk of anthropogenic climate change. Nat. Clim. Chang. 2021, 11, pp. 879–885.

[39] Bala, G. Caldeira, K. Wickett, M. Phillips, T.J.Lobell, D.B. Delire, C. Mirin, A. Combined climate and carbon-cycle effects oflarge-scale deforestation. Proc. Natl. Acad. Sci. USA 2007, 104, p. 655.

[40]Reynolds, J.C. Blackburn, G.J. Guallar-Hoyas, C. Moll, V.H.; Bocos-Bintintan, V. Kaur-Atwal, G. Howdle, M.D. Harry, E.L.;Brown, L.J. Creaser, C.S.; et al. Detection of Volatile Organic Compounds in Breath Using Thermal Desorption ElectrosprayIonization-Ion Mobility-Mass Spectrometry. Anal. Chem. 2010, 82, pp. 2139–2144.

[41]Dewulf, J. Van Langenhove, H. Wittmann, G. Analysis of volatile organic compounds using gas chromatography. TrAC Trends Anal. Chem. 2002, 21, pp. 637–646.

[42]Alwis, K.U. Blount, B.C. Britt, A.S. Patel, D. Ashley, D.L. Simultaneous analysis of 28 urinary VOC metabolites using ultra high-performance liquid chromatography coupled with electrospray ionization tandem mass spectrometry (UPLC-ESI/MSMS). Anal. Chim. Acta 2012, 750, pp.152–160.

[43] Jahangir, I.; Koley, G. Dual channel microcantilever heaters for selective detection and quantification of a generic mixture of volatile organic compounds. In Proceedings of the 2016 IEEE Sensors, Orlando, FL, USA, 2016, pp. 1–3.

[44]Leidinger, M. Sauerwald, T. Reimringer, W. Ventura, G. Schütze, A. Selective detection of hazardous VOCs for indoor air quality applications using a virtual gas sensor array. J. Sensors Sens. Syst. 2014, 3, pp. 253–263.

[45]Kanda, K. Maekawa, T. Development of a WO3 thick-film-based sensor for the detection of VOC. Sens. Actuators B Chem. 2005,108, pp. 97–101.

[46]Stegmeier, S. Fleischer, M. Hauptmann, P. Thermally activated platinum as VOC sensing material for work function type gas sensors. Sens. Actuators B Chem. 2010, 144, pp. 418–424.

[47]Fan, Z. Lu, J.G. Chemical Sensing with ZnO Nanowire. In Proceedings of the 5th IEEE Conference on Nanotechnology, Nagoya,Japan,2005.

[48]Janeiro, R. Flores, R. Viegas, J. Silicon photonics waveguide array sensor for selective detection of VOCs at room temperature.Sci. Rep. 2019, 9, 17099.

[49] Zhou, J. Al Husseini, D.Li, J.; Lin, Z.; Sukhishvili, S. Coté, G.L. Gutierrez-Osuna, R. Lin, P.T. Detection of volatile organic compounds using mid-infrared silicon nitride waveguide sensors. Sci. Rep. 2022, 12, 5572.

[50]Fernández, F. Hegnerová, K.Piliarik, M. Sanchez-Baeza, F. Homola, J. Marco, M.-P. A label-free and portable multichannelsurface plasmon resonance immunosensor for on site analysis of antibiotics in milk samples. Biosens. Bioelectron. 2010, 26, pp. 1231–1238.

[51]Elosua, C. Matias, I.R. Bariain, C. Arregui, F.J. Volatile Organic Compound Optical Fiber Sensors: A Review. Sensors 2006, 6, pp. 1440–1465.

[52]Park, C.-S. Han, Y. Joo, K.-I. Lee, Y.W. Kang, S.-W. Kim, H.-R. Optical detection of volatile organic compounds using selective tensile effects of a polymer-coated fiber Bragg grating. Opt. Express 2010, 18, pp. 24753–24761.

[53]Schweizer, G. Latka, I. Lehmann, H. Willsch, R. Optical sensing of hydrocarbons in air or in water using UV absorption in theevanescent field of fibers. Sens. Actuators B Chem. 1997, 38, pp.150–153.

[54]Shadaram, M. Espada, L. Martinez, J. Garcia, F. Modeling and performance evaluation of ferrocene-based polymer clad taperedoptical fiber gas sensors. Opt. Eng. 1998, 37, 1124.

[55]Barmenkov, Y.O. Ortigosa-Blanch, A. Diez, A.; Cruz, J.L. Andrés, M.V. Time-domain fiber laser hydrogen sensor. Opt. Lett. 2004,29, pp. 2461–2463.

[56] Lacroix, S. Bourbonnais, R. Gonthier, F.Bures, J. Tapered monomode optical fibers: Understanding large power transfer. Appl.Opt. 1986, 25, pp. 4421–4425

[57]Willer, U. Scheel, D. Kostjucenko, I. Bohling, C. Schade, W. Faber, E. Fiber-optic evanescent-field laser sensor for in-situ gasdiagnostics. Spectrochim. Acta Part A Mol. Biomol. Spectrosc. 2002, 58, pp. 2427–2432.

[58]Opliss, S. James, S. Davis, F. Higson, S. Tatam, R. Optical fibre long period grating based selective vapour sensing of volatileorganic compounds. Sens. Actuators B Chem. 2010, 143, pp. 629–634.

[59]Konstantaki, M.; Skiani, D.; Vurro, D.; Cucinotta, A.; Selleri, S.; Secchi, A.; Iannotta, S.; Pissadakis, S. Silk Fibroin Enabled OpticalFiber Methanol Vapor Sensor. IEEE Photon. Technol. Lett. 2020, 32, pp. 514–517.

[60] Soleymani, parviz, amini ranjbar, gh.r. separation and identification of organ chlorine and organ phosphorus compounds in the anzali lagoon water by gc/ms ion trap system. pajouhesh-va-sazandegi, 14(1 (50 in animal and fisheries sciences)),2001,pp.76-80. sid. https://sid.ir/paper/19735/en.

[61]H.N. Nayan Kumar,D.H. Nagaraju, Zhoveta Yhobu,P. Shivakumar , K.S. Manjunatha Kumara,Srinivasa Budagumpi ,B.M. Praveen,Recent advances in on-site monitoring of heavy metal ions in the environment,Microchemical Journal,Volume 182,2022, 107894, p.1.

[62] Viviana Scognamiglio, Amina Antonacci, Luisa Patrolecco, Maya D Lambreva, Simona C Litescu, Sandip A Ghuge, Giuseppina Rea Analytical tools monitoring endocrine disrupting chemicals TrAC Trends in Analytical Chemistry, 2016, Vol: 80, p. 555,

[63] Tatsuro Endo, Yasuko Yanagida, Takeshi Hatsuzawa, Photonic crystal based optical chemical sensor for environmental monitoring, 2007.

[64] TatsuroEndo, Yasuko Yanagida, Takeshi Hatsuzawa, Photonic Crystal based Optical Chemical Sensor for Environmental Monitoring, 2007, Hong Kong.

Chapter II: Photonic crystals: Analysis, design and sensing applications

II.1 Introduction

Photonic crystals are materials that have a periodic structure on the wavelength scale of light, allowing them to manipulate light in unique ways. This periodic structure creates gaps in the optical band, areas where certain wavelengths of light cannot propagate. By controlling these band gaps, photonic crystals can be used to precisely control the flow of light, making them highly valuable in various technological applications.

The analysis and design of photonic crystals involve sophisticated computational methods to predict and optimize their interactions with light. These methods allow the properties of photonic crystals to be tailored to achieve specific desired outcomes in applications ranging from telecommunications to sensing.

In sensing applications, photonic crystals are particularly promising due to their high sensitivity to changes in the environment. This sensitivity allows them to detect a wide range of stimuli, including biological molecules, chemicals, and environmental conditions. As a result, photonic crystals are being explored for use in advanced sensors for medical diagnostics, environmental monitoring, and chemical detection.

II.2 Photonic crystals: Past, present and future

Photonic crystals are optical nanostructures that exhibit periodic changes in refractive index, similar to how the atomic lattices in semiconductors affect electron conductivity. These structures have the potential to manipulate the propagation of light and find applications in various fields. In this article, we will explore the past, present, and future of photonic crystals.

Past: The study of photonic crystals dates back to 1887 when Lord Rayleigh conducted experiments on periodic multi-layer dielectric stacks, demonstrating the existence of a one-dimensional photonic band-gap [1]. Over the years, researchers made significant progress in understanding the properties and potential applications of photonic crystals. In 1987, Eli Yablonovitch and Sajeev John published milestone papers on high-dimensional periodic optical structures, which are now referred to as photonic crystals [1]. These papers sparked a surge of interest and research in the field.

Present: Currently, photonic crystals are being extensively studied and developed. They can be fabricated in one, two, or three dimensions using various techniques such as thin-film deposition, photolithography, drilling, direct laser writing, and self-assembly [1]. Photonic crystals have already found practical applications, such as dielectric mirrors for ultra-high reflectivity, photonic-crystal fibers for fiber-optic communication, and high-density photonic

integrated circuits [1]. Researchers are also exploring using photonic crystals in optical computers and more efficient photovoltaic cells [1].

Future: The future of photonic crystals holds great promise. Ongoing research aims to overcome fabrication challenges and explore new materials and structures. Opening up complete photonic band gaps is a key goal, which can be achieved by increasing the refractive index contrast or utilizing quasicrystalline structures [1]. Three-dimensional photonic crystals with face-centered cubic lattice structures and high-refractive-index semiconductor materials have demonstrated complete band gaps [1]. Additionally, using low-index polymer quasicrystalline samples manufactured by 3D printing has shown potential for achieving complete photonic band gaps [1]. These advancements pave the way for further applications in areas such as optical computing, advanced telecommunications, and energy harvesting.

Concept of photonic forbidden bands:

Photonic crystals (PhCs) are an engineered optical material represented by natural or artificial structures with periodic modulation of the refractive index. Photonic crystals are classified mainly into three categories, that is, one-dimensional (1D), two-dimensional (2D), and three-dimensional (3D) crystals according to the periodicity of dielectric material along one or more axes [10] as shown in Figure 1.

II.3 Concepts of Photonic Crystal

These structures have revolutionized the field of optics and photonics, allowing us to manipulate light in novel ways. Here is a concise overview of the concepts you have mentioned:

II.3.1 Periodic Structure and Dimensionality

A photonic crystal is a material with a periodic variation in refractive index. This periodicity can occur at the nanoscale, typically about the optical wavelength.

Just as the periodic lattice of crystalline solid results in electronic band gaps, a periodic dielectric structure gives rise to photonic band gaps (PBGs). These gaps in the photonic frequency spectrum prevent certain wavelengths of light from propagating through the crystal. The dimensionality of photonic crystals plays a crucial role. Common structures include :

1. 1D Photonic Crystals: Exhibit periodicity in one dimension (e.g., layered structures).
2. 2D Photonic Crystals: Have periodicity in two dimensions (e.g., square or hexagonal lattices).

3. 3D Photonic Crystals: Extend the periodicity into three dimensions (e.g., diamond-like structures).

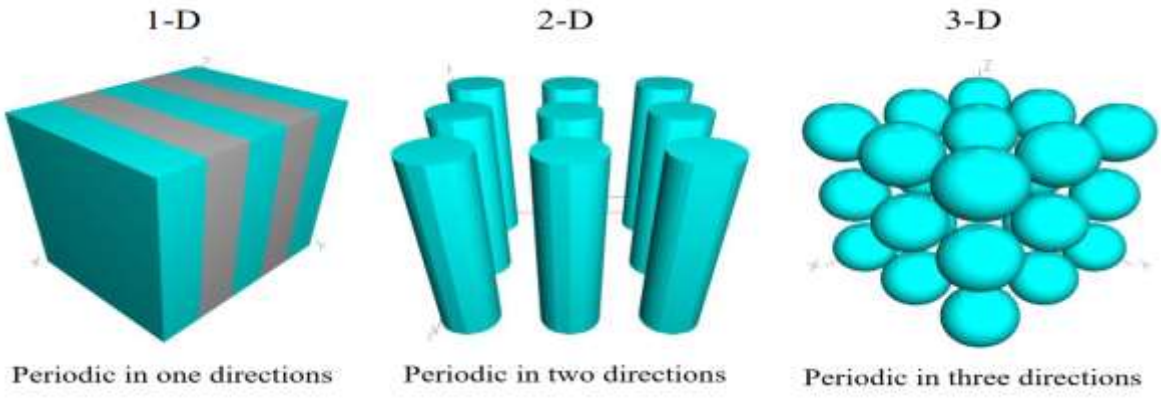

Figure II 1Representation of one, two, and three-dimensional photonic crystals[2].

II.3.2 Photonic Band Gaps and Wave Propagation

The concept of band structure applies to photonic crystals. Just as electrons in a solid experience energy bands and band gaps, photons in a photonic crystal encounter photonic bands and band gaps.

The photonic band gap arises from coherent scattering of light within the periodic structure. When the wavelength of light matches the periodicity of the crystal, destructive interference occurs, leading to a gap in allowed energy states.

Within the band gap, certain frequencies of light cannot propagate through the crystal. This property is exploited for controlling light in various applications.

II.3.3 Interaction with Electromagnetic Waves

Photonic crystals can be engineered to exhibit specific properties:

Waveguides: are channels within the crystal that guide light along specific paths.

Cavities and Defects: By introducing engineered defects (e.g., missing lattice sites), we create localized modes that trap light.

Superprism Effect: Photonic crystals can exhibit large angular dispersion, allowing for efficient wavelength separation.

Negative Index Materials: Some photonic crystals exhibit negative refraction, leading to intriguing optical effects.

II.4 Modelling of Photonic Structures

II.4.1 The plane wave expansion method (PWM)

The plane wave expansion method (PWM) is a computational technique used in electromagnetics to solve Maxwell's equations by formulating an eigenvalue problem [3]. It is commonly employed in physics and engineering, particularly in the field of photonics, to analyze structures such as photonic crystals, Bragg arrays, and micro-structured fibers [4].

a) Working Principle: We start with the periodic dielectric structure (the photonic crystal) and assume that the electromagnetic field can be represented as a superposition of plane waves. By solving Maxwell's equations, we find the dispersion relation (energy vs. wave vector) for different modes (bands) within the crystal.

   The band structure reveals allowed and forbidden energy states, analogous to electronic band gaps.

b) Advantages:

   Suitable for periodic structures.

   Provides detailed information about band gaps and modes.

   Can handle anisotropic materials.

c) Limitations:

   Requires solving eigenvalue problems numerically.

   Assumes infinite crystal size (boundary effects are neglected).

II.4.2 Finite-difference time-domain method (FDTD)

The FDTD method was originally proposed by Kane S. Yee in 1966. Yee de rives a complete three-dimensional formulation, and he validated the method with problems two-dimensional. Yee's method has been mostly unnoticed for nearly a decade. Finally, in 1975, Taflove and Brodwin applied Yee's method to simulate diffusion by dielectric cylinders. The FDTD (Finite Difference Time Domain) method is particularly interesting to know the spectral response of a system not necessarily periodic and to calculating field distributions in finite-dimensional structures. She does notrequire an initial hypothesis about the possible form of solutions or waves propagating in the structure, which makes it independent of the geometry of the systemto model. It is based on the temporal and spatial discretization of the equations of Maxwell by replacing the partial derivatives by their Taylor expansion at order 2,that is to say by finite differences. The main disadvantage of FDTD, which, however, tends to fade with developments in IT capabilities, is that it is very slow and requires significant computer resources[5].

Principle: The FDTD method is a volume-based method that requires dividing the solution space into a uniform mesh composed of cells. In each cell, the components of the fields E and H are defined. This aspect of the FDTD method is similar to FEM. However, in FEM, a matrix equation is developed, which can then be solved in various ways. In the FDTD method, no matrix solution is necessary. In other words, as time progresses, the solution for each field component is determined for that particular instant in time and then stored in memory. The development of FDTD here will be based on the Yee cell. The peculiarity of the Yee cell is that the field components are staggered E.and H are shifted by half a spatial cell, which facilitates the diagrams of differentiation that are sufficiently precise[6].

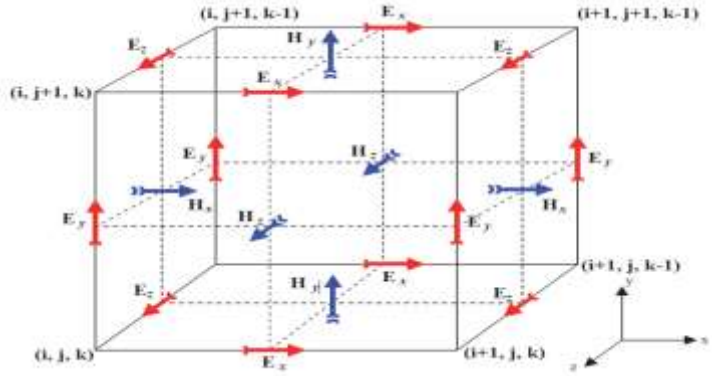

Figure II 2Diagram of a Yee cell (3D FDTD discretization). The electric field vectors E are positioned on the edges and the magnetic field vectors H at the center of the faces of the cell. (Vitale, 2014) [7].

In 1865, James Clerk Maxwell developed the theoretical laws of classic electrodynamics. He claimed that light itself was an electromagnetic phenomenon, and postulated electric and magnetic fields are related to each other and their enclosing media in space and time. The combinations of several laws in a unified notation are collectively known as Maxwell's equations. Time-dependent Maxwell's equations are given in differential form as Faraday's Law, Ampere's Law , Gauss's Law for electric field and Gauss's Law for magnetic field [8].

$$\nabla . \overrightarrow{H}(\vec{r}, t) = 0 \quad (I.1)$$

$$\nabla . \varepsilon(\vec{r}) \overrightarrow{E}(\vec{r}, t) = 0 \quad (I.2)$$

$$\nabla \times \overrightarrow{E}(\vec{r}, t) = -\frac{\partial \vec{B}}{\partial t} \quad (I.3)$$

$$\nabla \times \overrightarrow{H}(\vec{r}, t) = -\frac{\partial \vec{D}}{\partial t} \quad (I.4)$$

II.4.3 Boundary conditions (PML)

Boundary conditions, specifically Perfectly Matched Layers (PML), are used in numerical methods to simulate problems with open boundaries. PML is commonly used in methods such as Finite-Difference Time-Domain (FDTD) and Finite Element (FE) to truncate computational regions and minimize reflections at the boundaries [9].

PML is an artificial absorbing layer that is designed to absorb outgoing waves from the interior of a computational region without reflecting them into the interior [8]. It achieves this by implementing an absorbing material that is impedance-matched to the surrounding materials, reducing reflections. The goal of PML is to create a boundary that produces minimal reflections, although, in practice, there may still be small reflections due to the discretization of the underlying PML equations [9].

The key property of PML is that waves incident upon the PML from a non-PML medium do not reflect at the interface. This property allows the PML to strongly absorb outgoing waves without reflecting them back into the computational region [9]. PML can be seen as an artificial anisotropic absorbing material that attenuates propagating waves and accelerates the attenuation of evanescent waves [10].

- **Perfectly matched layer (PML) (Split field)**

a) Boundary Conditions (Perfectly Matched Layers, PML):

   When simulating photonic structures, we need appropriate boundary conditions to prevent reflections at the computational domain edges.

b) Perfectly Matched Layers (PML):

   PML is an absorbing layer added around the simulation domain.

   It gradually absorbs outgoing waves, preventing reflections.

   PMLs are essential for accurate FDTD simulations.

c) Advantages:

Reduces artificial reflections.

Improves accuracy near boundaries.

d) Limitations:

Requires careful tuning of PML parameters.

May increase computational cost.

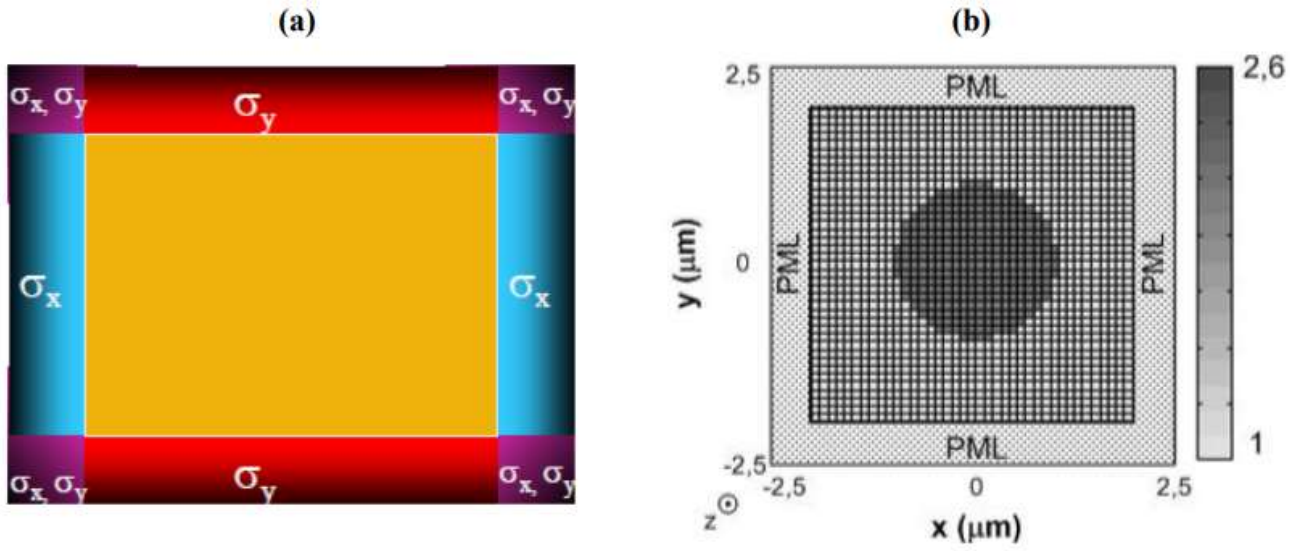

Figure II 3Use of PML layers (a) in the 2D case (b) Example of a mesh of a circular structure with application of PML boundary conditions

II.5 fabrication Process

II.5.1 Silicon-On-Insulator (SOI) Platform

SOI is a semiconductor fabrication technique that offers several advantages over conventional bulk silicon substrates. Here's what you need to know:

1. **The SOI**
    - Silicon on insulator (SOI) refers to the use of a three-layered substrate instead of conventional bulk silicon substrates.
    - The structure consists of the following layers:
        - Active Layer: A thin layer of prime-quality silicon (also known as the device layer)[11].
        - Buried Oxide Layer (BOX): An electrically insulating layer made of silicon dioxide (SiO_2) that isolates the active layer from the substrate.[11]

- Bulk Silicon Support Wafer (Handle): The underlying silicon substrate that provides mechanical support[11].

Advantages of SOI: SOI technology offers several benefits compared to traditional bulk silicon processing

- Lower Parasitic Capacitance: The insulating layer (BOX) reduces parasitic capacitance within the device, leading to improved power consumption and performance[12].
- Resistance to Latchup: Complete isolation of the n-well and p-well structures prevents latchup[12].
- Higher Performance at Equivalent VDD: SOI devices can operate at lower supply voltages (VDD) while maintaining performance[12].
- Reduced Temperature Dependency: SOI devices exhibit less temperature sensitivity due to the absence of doping effects[12].
- Better Yield and Wafer Utilization: High density and improved wafer utilization contribute to better yield[12].
- Lower Leakage Currents: Isolation results in higher power efficiency[12].
- Inherent Radiation Hardening: SOI devices are resistant to soft errors, reducing the need for redundancy[12].

2. **Manufacturing Considerations**

- SOI substrates are compatible with most conventional fabrication processes, requiring minimal retooling[12].
- Challenges include novel metrology for the buried oxide layer and concerns about differential stress in the topmost silicon layer[12].
- The threshold voltage of SOI transistors depends on their operational history and applied voltage, making modeling more complex[12].
- The primary barrier to SOI implementation is the increased substrate cost, contributing to manufacturing expenses[12].

3. **Fully Depleted Silicon on Insulator (FD-SOI)**

- FD-SOI is a planar process technology that simplifies manufacturing while delivering the benefits of reduced silicon geometries[12].
- Tight electrostatic control of transistors and innovative power management techniques characterize FD-SOI[12].

In summary, SOI technology enables higher-performing, lower-power devices and plays a crucial role in semiconductor miniaturization

II.5.2 Wafer chip preparation

During the wafer manufacturing process, wafer products are inspected at different points to detect any defects caused by the manufacturing process. This is essential in order to remove any substandard wafer materials and categorize the wafers into groups of consistent thickness. Ultimately, the wafers undergo a final inspection before being used as the primary raw material for creating new integrated circuits. The steps involved in a standard wafer manufacturing process are outlined below[13].

Crystal Growth and Wafer Slicing Process

The first step in the wafer manufacturing process is the formation of a large, perfect silicon crystal. The crystal is grown from a 'seed crystal' that is a perfect crystal. The silicon is supplied in granular powder form, and then melted in a crucible. The seed is immersed carefully into the crucible of molten silicon, and then slowly withdrawn.

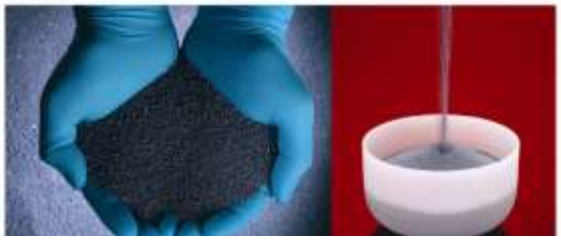

Figure II 4 Crystal Growth Efficiency with Fluidized Bed Reactor-Produced Granular Polysilicon. [14]

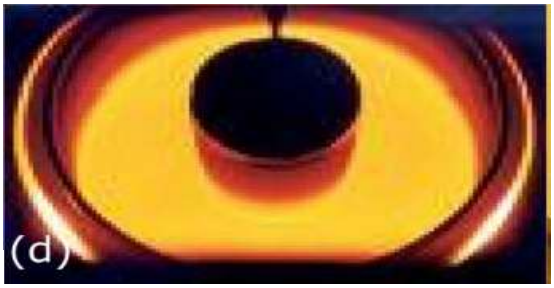

Figure II 5 shoulder [14]

Step 1: Obtaining the Sand:

The sand used to grow the wafers has to be a very clean and good form of silicon. For this reason not just any sand scraped off the beach will do. Most of the sand used for these processes is shipped from the beaches of Australia[13].

- **Step 2: Preparing the Molten Silicon Bath:**

The sand (SiO2) is taken and put into a crucible and is heated to about 1600 C° – just above its melting point. The molten sand will become the source of the silicon that will be the wafer[13].

- **Step 3: Making the Ingot:**

A pure silicon seed crystal is now immersed in the molten sand bath and slowly pulled out while being rotated. This process, known as the Czochralski (CZ) method, produces a pure silicon cylinder known as an ingot[13].

Figure II 6 The Czochralski method [15].

This step is done to provide a good clean surface for later processing. If a layer of Silicon is grown onto the top of the wafer using chemical methods then that layer is of a much better quality than the slightly damaged or unclean layer of silicon in the wafer. The epitaxial layer is where the actual processing will be done.

- The diameter of the silicon ingot is determined by the temperature variables as well as the rate at which the ingot is withdrawn. When the ingot is the correct length, it is removed, and then ground to a uniform external surface and diameter.
- Each of the wafers is given either a notch or a flat edge that will be used later in orienting the wafer into the exact position for later procedures[13].

- **Step 4: Preparing the Wafers:**

After the ingot is ground into the correct diameter for the wafers, the silicon ingot is sliced into very thin wafers. This is usually done with a diamond saw.

Each of these wafers will then go through polishing until they are very smooth and just the right thickness[13].

There are five stages in this step:

- Thickness Sorting

- Lapping & Etching Processes
- Thickness Sorting and Flatness Checking
- Polishing Process
- Final Dimensional and Electrical Properties Qualification

II.5.3 Device Patterning

Device patterning plays a crucial role in the fabrication of photonic crystals, which are optical materials with periodic variations in refractive index. These periodic structures enable precise control over the flow of light and find applications in various fields such as optical fibers, sensors, and lasers.

- **Electron Beam Lithography:**

One method used for patterning photonic crystal structures is electron beam lithography. This technique involves modifying a scanning electron microscope to create patterns with high precision and resolution.

- **Pattern-Integrated Interference Lithography (PIIL):**

Another approach is the use of pattern-integrated interference lithography (PIIL). This technique involves simulating the fabrication process of photonic crystal devices and calculating their transmission spectra. The performance of PIIL-produced devices is comparable to their idealized counterparts.

- **Direct Writing:**

Direct writing is an important and convenient method for fabricating patterned photonic crystals. By using properly dried polymer films as "paper" and dispersions of spheres as "inks," the self-assembly of spheres and locking of the photonic crystal structure can be achieved simultaneously. This results in tough composite patterned photonic crystals with uniform, stable, and permanent structural colors.

- **Advantages of Device Patterning:**

Device patterning allows for the precise control and manipulation of light propagation in photonic crystals. By creating periodic variations in refractive index, specific optical properties can be achieved, such as bandgaps that prohibit certain wavelengths of light from passing through the crystal structure.

II.5.4 Process flow for fabrication of alignment markers

- **Design and Layout:**

Begin by designing the alignment markers. Consider their size, shape, and placement.

Use software tools (such as AutoCAD or other design software) to create the layout. Ensure that the markers are compatible with the overall device or structure.

- **Substrate Preparation:**

Choose an appropriate substrate material. Common choices include silicon, glass, or polymer.

Clean the substrate thoroughly to remove any contaminants.

Deposit a thin layer of material (e.g., silicon dioxide) on the substrate to serve as the alignment marker base.

- **Photolithography:**

Apply a photoresist layer onto the substrate.

Expose the photoresist to UV light through a photomask containing the alignment marker pattern.

Develop the photoresist to reveal the desired marker pattern.

- **Etching:**

Use wet or dry etching techniques to transfer the marker pattern from the photoresist to the substrate.

Etch away the exposed areas of the substrate to create the alignment markers.

- **Inspection and Quality Control:**

Inspect the alignment markers under a microscope to ensure their accuracy and integrity.

Measure their dimensions and alignment precision.

- **Integration:**

Incorporate the alignment markers into the final device or structure. For photonic crystals, this could involve integrating them into the photonic crystal lattice.

- **Testing:**

Validate the alignment markers' functionality by performing alignment tests.

Ensure that they aid in precise positioning during subsequent processes (e.g., lithography, deposition, or bonding).

II.6 Application of PhCs

II.6 .1 Photonic crystal waveguide (PhCW)

Linear waveguides are crucial for integrated photonic circuitry, relying on the refractive index contrast between the waveguide core and cladding. Photonic crystal waveguides are often structured with a linear defect, comprising modified unit cells in a high-index dielectric membrane, facilitating guidance through total internal reflection at the membrane/cladding interfaces and distributed reflections from the photonic crystal. This mixed confinement enables

minimal transmission loss in small bending radius waveguide branches and bends, as demonstrated experimentally. Consequently, photonic crystal waveguides are promising for densely integrated photonic circuits due to their capability to support small bending radii with near-total transmission[16].

(a) (b)

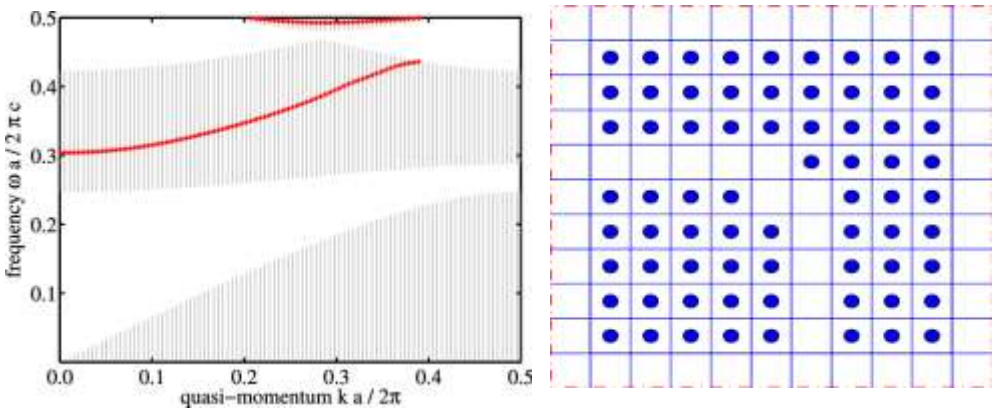

Figure II 7 A/Simulated band diagram for W1 straight PhCW and the corresponding supercell Inset show the magnetic-like field profiles for (a) odd mode and (b) even mode. B/A 90◦ PhC waveguide bend in a finite PhC consisting of circular dielectric rods on a square l

II.6 .2 PhC cavities (PhCC)

In 1989, PhC cavities incorporating two Bragg reflection distributions were first introduced. However, the concept of a forbidden optical band was introduced in 1987, predating the appearance of a vertical cavity. Essentially, a laser cavity serves as a containment vessel that can trap photons within a limited space for extended durations. PhC cavities can confine photons within very small spaces, with the potential for very high-quality factors, making them appealing for laser applications. These cavities can be formed within the band gap range. Defect modes within the bandgap region arise from anomalies in the PhC structure. Allowed modes within the forbidden electromagnetic band in a PhC sheet are created by one or more defects, which disrupt the periodic crystal structure. This phenomenon is akin to the formation of deep levels in the electronic forbidden band of a solid, caused by impurities. [19]

II.6 .3 Optical properties and sensing principles of PhCCs

- **Nature of Optical Fields**

Optical fields refer to the distribution of electromagnetic energy in space. They are characterized by their wavelength, frequency, and polarization.

PhCCs manipulate optical fields by creating periodic structures that interact with light in specific ways. These structures exhibit bandgaps, where certain wavelengths are forbidden, allowing precise control over light propagation.

- **Properties of Optical Materials**

The success of PhCCs relies on the interplay between optical fields and materials.

Key material properties include refractive index, dispersion, absorption, and scattering. These properties determine how light interacts with the material.

PhCCs are often fabricated using materials with tailored optical properties to achieve desired effects.

- **Sensing Principles Based on PhCCs**

PhCs can be employed in various sensing applications due to their unique optical behavior:

Electrical External Signal Sensors:

These sensors respond to external electrical signals. For instance: PhCCs integrated with liquid crystals (LCs) can detect changes in an applied electric field.

LCs alter their refractive index based on the electric field, affecting the PhCC's band structure.

Electrochemical Sensors:

PhCCs can also sense electrochemical changes in their surroundings. For example, variations in the refractive index due to chemical reactions or analyte binding can modify the PhCC's bandgap properties.

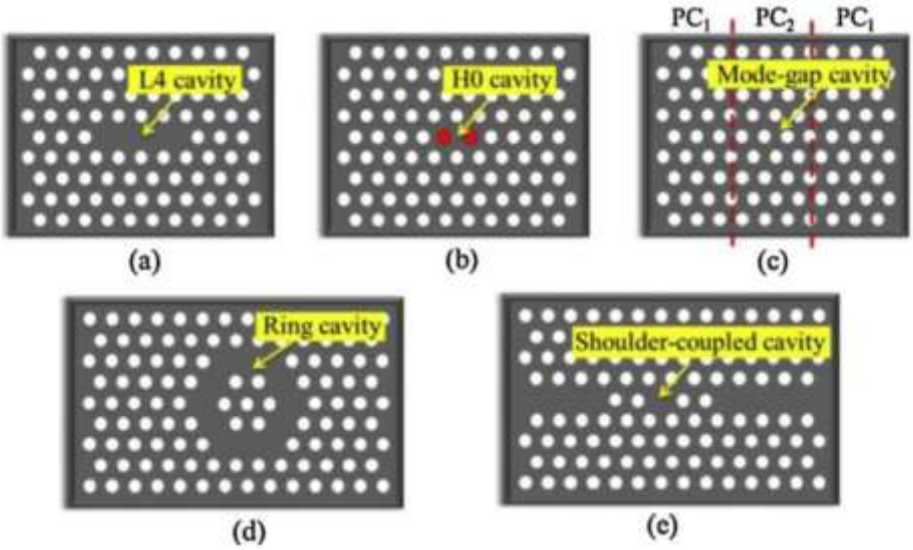

Figure II 8 Schematic structures of (a) L4 PhCC, (b) H0 PhCC, (c) mode-gap PhCC, (d) ring hCC, and (e) shoulder-coupled PhCC [20].

By monitoring these changes, PhCCs become sensitive to specific analytes or environmental conditions.

II.6 .4 Optical sensors based on PhCs

Recently, there has been an increased interest in developing optical sensors for a variety of sensing applications, thanks to their unique advantages,such as resistance to electromagnetic interference, small size, lightweight, wide bandwidth, environmental durability, and low attenuation. Photonic Crystal (PhC) based sensors have shown great promise due to their ability to trap light in complex ways and their compact structure. Photonic crystals have become a focus of interest for biological and chemical detection due to their ability to control the interaction between matter and electromagnetism. They can be used to trap light in a region with a low refractive index, providing suitable conditions for strong interaction sensing applications. Between light and matter, thus achieving high sensitivity. Typically, sensors based on photonic crystals are characterized by a very sharp resonant peak, which reduces the

detection limits, leading to strong dispersive phenomena and long photon storage time. This unique feature makes these structures compact and an attractive platform for refractive index-based sensing applications[21].

II.6 .4 .1 PhCW sensors

The primary function of PhCW sensors is to confine the electromagnetic field of radiation within specific rows of holes in order to maximize the interaction of the beam with the small amount of sample present in those holes. In a two-dimensional PhCW, a liquid or gas flows through the holes while the propagation of a beam is observed for any changes induced by the sample. One way to create a PhCW is by removing the air holes in a single row. It is crucial to have a low group velocity and high transmission in order to support a propagating mode in the PhCW. Monitoring the changes in the transmission spectrum of the sample that has infiltrated the air holes in the line defect is essential to ensure the effectiveness of the material-electromagnetic field interaction[21].

II.6 .4 .2 Gas sensors based on PhCs

Optical sensors have become a promising device for gas sensing due to their immunity to electromagnetic interference (EMI), rapid response time, room temperature operation, and offline monitoring features. The integration of microfluidics with Photonic Crystal (PhC) technologies has led to the development of proper gas sensors. This integration promotes optical sensors with high sensitivity, a good limit of detection, and detection multiplexing capability.

The most commonly used technique for optical gas sensing is absorption spectroscopy, which is highly sensitive but requires a long absorption length. The light confinement feature of PhCs enhances the light-matter interaction, resulting in the development of their sensitivity characteristic.

In 2011, Awad et al. proposed a PhC waveguide-based gas sensor for detecting Argon and Helium gases. They observed a shift in cutoff wavelength of 0.6 nm and 0.05 nm for Argon and Helium gases, respectively. The interaction between the gas infiltrated in the structure and the slow-light mode propagation leads to changes in the slow-light regime wavelength, which is transduced by waveguide effective refractive index changes. In 2012, Zhao et al. reported a technique that combines harmonic detection signal processing with PhC slow-light waveguide technology for gas sensing. Kumar et al. proposed a PhC-based bi-periodic waveguide structure in which an array of super-cavities is used to pass the resonance wavelength through the waveguide. Goyal et al. proposed a PhC waveguide structure based on a ring-shaped PhC for gas sensing applications. The enhancement in sensitivity is achieved due to the enhancement of the guided mode near the core-cladding interface. Benelarbi et al. reported an improved sensitivity by selectively infiltrating adjacent two rows of PhCs.

In all the discussed PhC waveguide structures, light is confined in high refractive index (RI) materials. However, it is also possible to achieve light confinement in low RI materials by introducing an air-slot within the PhC waveguide structure, which has high potential for sensing applications[21].

Due to their ability to detect low concentration gaseous species, PhC-based sensors have been extensively researched for gas sensing applications. The characteristic parameters in gas sensing applications include quality factor, sensitivity, mode volume, and signal strength. The mode volume and quality factor are proportional to the size of the cavity and the energy stored inside the cavity structure, respectively. Sensitivity is also proportional to the quality factor. The optical mode in the waveguiding medium must be large enough to achieve a high quality factor[21].

II.6 .4 .3 Refractive index sensor based on PhCs

1. Photonic Crystal Fiber (PCF) with Elliptically Split Cores:
    - Researchers have developed an advanced refractive index sensor using a photonic crystal fiber (PCF) with elliptically split cores .
    - Here’s how it works :

- The PCF has two cores formed by an elliptical air hole at the center. These cores represent two independent waveguides.

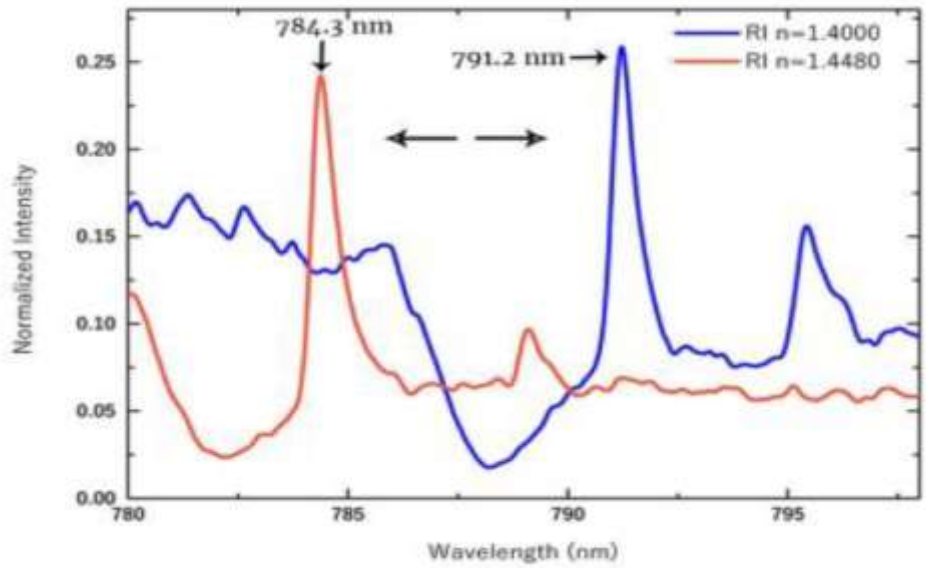

Figure II 9 Resonance wavelength shift corresponding to two different indices; n = 1.4000 and n = 1.4480. the resonance is highly sensitive to the refractive index of the fluids over the PhC and this involves a rapid change of the peak position [22].

- The elliptical shape of the air holes within the cladding allows for maximum sensitivity.
- The sensor's performance is investigated using a full-vector Finite Element Method technique.
- The proposed PCF-based sensor achieves maximum sensitivities of 9000 nm/RIU (for x-polarized light) and 10,000 nm/RIU (for y-polarized light).
- The sensing range of the analyte is 1.35–1.39.
- This sensor demonstrates excellent sensitivity and can detect various chemicals, cancer-causing agents, biomolecules, and other analytes.

2. Circular Photonic Crystal (CPC) Refractive Index Sensor

- Another intriguing design involves a circular photonic crystal (CPC) .
- Key features :
  - The CPC consists of a silicon ring surrounding a cavity.
  - The CPC's bandgap is determined from its transmission spectra.
  - By modulating the refractive index of the surrounding medium, the CPC can sense changes in the environment.

- Relationships between the sensor's performance parameters and its structure parameters are thoroughly investigated.

II.6 .4 .4 Surface wave sensor based on PhCs

Most sensors based on PhC technology rely on either the photonic stop band or the properties of Bragg reflection. However, some sensors utilize the surface wave on the periodic structure for sensing purposes. Villa et. al used such a sensor to analyze thin films. This sensor offers higher sensitivity compared to surface-plasmon polarization waves on a metallic surface. TE polarization is more effective for sensing applications, especially when TM polarization has the Brewster angle at a specific angle of incidence. The photonic band structure of 1D PhC is illustrated in Figure II.11. The dispersion curve for surface waves, calculated using the supercell method, only appears in the 1st and 3rd band gaps, as indicated by the dashed lines in the figure [21].

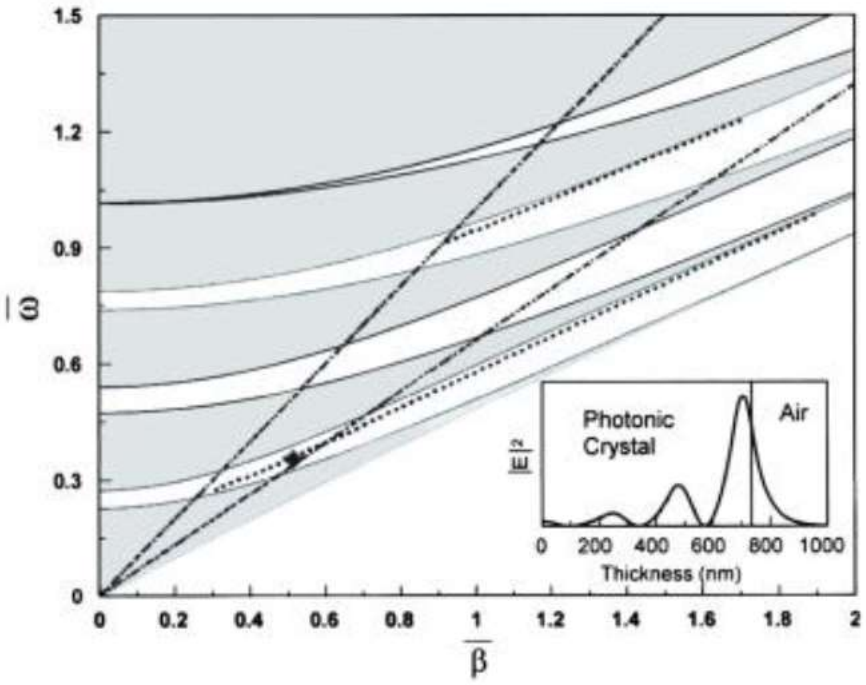

Figure II 10 Band Structure of TE polarization. The light lines for glass and vacuum at the angle of incidence of 85° are given by lower and upper dashed lines, respectively. The area limited by these lines presents the region where it is possible to excite surface

II.6 .4 .5 Biochemical sensors based on PhCs

The concentration of the biochemical sample is directly related to the refractive index (RI) of the alloy, making RI the main mechanism for measuring biochemical sensors through analytical interaction with an optical field. The effectiveness of a biochemical sensor depends

on various factors such as sensitivity, efficiency, miniaturizability, low latency, manufacturability, and cost-effectiveness. Recent configurations of biochemical sensors include photonic crystal fiber (PhC) sensors, where the electric field is confined in the core region surrounded by air holes for sample measurement. However, the sensitivity of these sensors is often low due to the rapid decay of the electromagnetic field in the sensing region. To improve sensitivity, longer PhC fibers can be used, but this may lead to issues such as increased sample quantities, greater latency, and uniform diffusion within the air holes.

PhC-based RI sensors have been developed to enhance sensitivity, with several PhC-based biochemical sensors introduced. In 2005, Chakravarty et al. used a PhC coated ion-selective polymer to measure cation and anion concentrations. Increasing the length of the cavity in PhC structures can enhance the Q factor and improve the shift of resonant wavelength while maintaining compact size characteristics. In 2007, Lee et al. demonstrated the ability of a PhC resonator with a single point defect to detect small protein molecules, gold nanoparticles, or anti-biotin in a low active sensing volume. Finally, in 2010, Hsiao et al. showed that a ring PhC is highly sensitive in controlling reaction kinetics and detecting low concentrations of proteins [21].

II.6 .4 .6 Temperature sensor based on PhCs

Temperature sensors can utilize PhCs. The fundamental idea behind a temperature sensor is to observe a change in the Bragg peak or photonic stop band as the temperature of the material in the PhC changes. PhCs are typically created using SiO2 spheres produced through sol-gel chemistry. The optical characteristics of the PhC alter when the refractive index (RI) changes. Therefore, if the RI fluctuates with temperature, the PhC can function as a temperature sensor [21].

II.6 .4 .7 Oil sensor based on PhCs

Oil sensing utilizes carbon-based inverse opals. The color change of the inverse opal can be easily seen with the naked eye when it comes into contact with oils. PhC-based oil sensors typically have a response time that is 30 seconds longer compared to other types of oil sensors. The regeneration efficiency of the inverse opal for diesel and its cyclic absorption performance are illustrated in Figure 2-12. The device remained stable for nine cycles, similar to other oils, with the same amount of oil being recovered as was absorbed in each cycle[21].

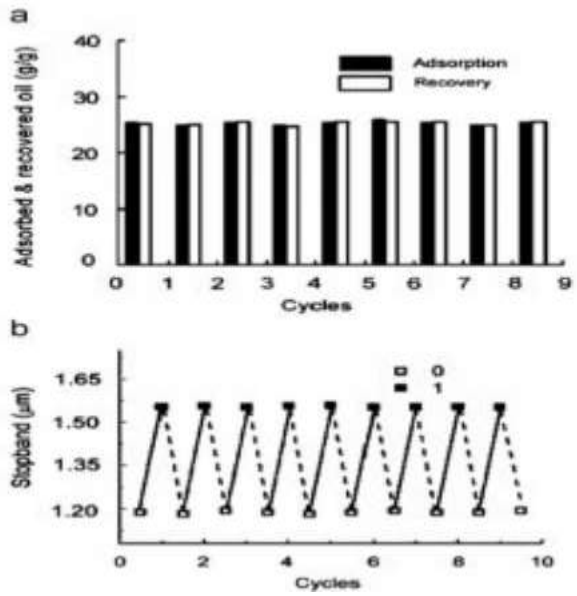

Figure II 11 Recycling performance of the PR inverse opal (a) Mass recycling efficiency. (b) Stop band position cycling. 0 and 1 represented the status of the PR inverse opal before and after oil sorption, respectively [24].

II.6.4 .8 Humidity sensor based on PhCs

PhCs made with a soft hydrogel can be used to detect changes in humidity levels in the environment by being directly exposed to the surrounding atmosphere. These sensors have a quick response time, typically in seconds, as they are thin films and are suitable for use in specific environments. Their compact size and flexibility make them appealing for applications where other sensors may not be suitable[21].

II.7 Conclusion

Photonic crystals (PhCs) represent a significant advancement in the fields of optics and photonics due to their ability to control light propagation through their periodic structures. This chapter covered the evolution of PhCs from theoretical foundations to practical applications, highlighting key modeling methods such as the plane wave expansion method (PWM) and the finite-difference time-domain method (FDTD), as well as the importance of boundary conditions (PML).

The detailed fabrication process of PhCs was discussed, with a focus on the Silicon-On-Insulator (SOI) platform and the precise steps required for wafer preparation and device patterning. Applications of PhCs were explored, emphasizing photonic crystal waveguides (PhCWs) and cavities (PhCCs) and their roles in enhancing sensor performance.

The applications of PhC-based optical sensors were reviewed, including various types such as gas sensors, refractive index sensors, biochemical sensors, temperature sensors, oil sensors, and humidity sensors. Each type leverages the unique properties of PhCs to achieve high sensitivity and accuracy.

In conclusion, PhCs offer great potential for developing advanced and precise sensing technologies. With ongoing research and development, we can expect further innovations that will enhance our ability to detect, measure, and analyze with exceptional efficiency.

Refrences:

[1] Photonic crystal - Wikipedia

[2] M. Maache, “Design and Optical Studies of Photonic Components Using Slow Light Properties,” Doctoral Dissertation, Faculty of Technology, Department of Electronic, University of Mohamed Boudiaf - M’sila, 2018/2019.

[3] Plane wave expansion method - Wikipedia

[4] The Bianisotropic Formulation of the Plane Wave Method from Faraday’s and Ampere’s Laws

[5] KOULLAL Amina,Contribution à la résolution numérique des équations de Maxwell dans le domaine temporel-application à la propagation des Ondes électromagnétiques dans les fibres à cristaux photoniques,MASTER EN PHYSIQUE,Spécialité:Physique Computationnelle,FACULTE DES SCIENCES – DEPARTEMENT DE PHYSIQUE ,UNIVERSITE ABOU-BEKR BELKAID - TLEMCEN,2020/2021 PAGE 29

[6] A. Labbani, «Matériaux bip a base de nanoparticules métalliques et semi-conductrices étude des propriétés optiques par FDTD» Thèse de doctorat, *Laboratoire Hyperfréquences et Semi-conducteurs, Université de Constantine, Algérie(2009).

[7] Cécile Finco, Study of the simultaneous impact of electrical, dielectric and magnetic properties of the subsurface on geophysical measurement by inductive electromagnetic method in the time domain (TDEM), Thèse de doctorat de Géophysique appliquée, École doctorale Géosciences, Ressources Naturelles et Environnement (ED 398) UMR 7619 METIS, Sorbonne Université , October 2019, page 57

[8] Abdul Rahman, M. G. (2017). *1D photonic crystal nanocavities for optical sensing* (Doctoral dissertation, University of Glasgow).

[9] S. D. Gedney and B. Zhao, “An Auxiliary Differential Equation Formulation for the Complex-Frequency Shifted PML,” IEEE Trans. on Antennas & Propagat., vol. 58, no. 3, 2010.

[10] Perfectly matched layer – Wikipedia

[11] M. Notomi, “Manipulating light with photonic crystals,” *Rep. Prog. Phys.*, vol. 73, no. 9, 096501, September 2010.

[12] "Silicon on insulator," Wikipedia, the free encyclopedia, https://en.wikipedia.org/wiki/Silicon_on_insulator (accessed May 29, 2024).

[13] Dr. Seth, P. Bates," Silicon Wafer Processing", Summer, 2000, page3

[14] Graham R. Fisher, Mike Seacrist, "Silicon Crystal Growth and Wafer Technologies" Article in Proceedings of the IEEE, May 2012.

[15] ollia nttila,"manufacture of high resistivity low oxygen czochralski silicon,jone 2005,page 8

[16]J. O'Brien,W. Kuang, Encyclopedia of Modern Optics,PHOTONIC CRYSTALS | Photonic Crystal Lasers, Cavities and Waveguides, University of Southern California, Los Angeles, CA, USA,28 May 2005,page 146-155

[17] Din Chai Tee,Muhammad Hafiz Abu Bakar,Faisal Rafiq Mahamd Adikan, Faisal Rafiq Mahamd Adikan,High-Transmission-Efficiency 120 Photonic Crystal Waveguide Bend by Using Flexible Structural Defects,Article in IEEE Photonics Journal,20 August 2014,page6

[18] Jianhua Yuan,Ya Yan Lu,Dirichlet-to-Neumann Map Method with Boundary Cells for Photonic Crystals Devices,Article in Communications in Computational Physics, January 2011, page4

[19] Mohammad Javad Safdari,Design, analysis, and optimization of photonic crystal Sensors, Master of Applied Science, Faculty of Engineering and Computer Science,The Department of Electrical and Computer Engineering,Concordia University,June 2018,page21

[20]Y.-N. Zhang, Y. Zhao, D. Wu, and Q. Wang, “Fiber Loop Ring-Down Refractive Index Sensor Based on High-$ Q $ Photonic Crystal Cavity,” IEEE Sens. J., vol. 14, no. 6, pp.1878–1885, 2014.

[21] Mohammad Javad Safdari, Design, analysis, and optimization of photonic crystal Sensors, Master of Applied Science, Faculty of Engineering and Computer Science,The Department of Electrical and Computer Engineering, Concordia University, June 2018,page21

[22] Y.-N. Zhang, Y. Zhao, D. Wu, and Q. Wang, “Fiber Loop Ring-Down Refractive Index Sensor Based on High-$ Q $ Photonic Crystal Cavity,” IEEE Sens. J., vol. 14, no. 6, pp. 1878–1885, 2014.

[23]F. Hsiao and C. Lee, “Computational study of photonic crystals nano-ring resonator for biochemical sensing,” IEEE Sens. J., vol. 10, no. 7, pp. 1185–1191, 2010.

[24]F. Hsiao and C. Lee, “Computational study of photonic crystals nano-ring resonator for biochemical sensing,” IEEE Sens. J., vol. 10, no. 7, pp. 1185–1191, 2010.

Chapter III:Results and discussions

III.1. Introduction

Optique Sensors refer to a class of sensing devices that operate based on optical principles, utilizing light as the detection mechanism. These sensors leverage the unique properties of light-matter interactions to detect and quantify various physical, chemical, or biological quantities of interest.

A photonic crystal gas sensor is a type of optical sensor that utilizes photonic crystals, which are nano-structured materials with a periodic variation in their refractive index, to detect the presence and concentration of specific gases.

The purpose of this chapter is to explain the operating principle of this type of sensor, propose designs for photonic crystal-based gas sensors for optical detection of toxic gases, and optimize the proposed structures to improve optical detection performance.

III.2. Mechanism detection of Toxic Gas sensor based on Photonic Crystalstucture

Photonic crystal (PC) sensors leverage the phenomena of light-matter interactions to detect the presence of target gas molecules. When gas molecules are adsorbed onto the surface of the photonic crystal, they cause a change in the refractive index of the material. This change in refractive index alters the transmission and reflection characteristics of the photonic crystal, which can be detected and analyzed to determine the type and concentration of the gas present.

The specific mechanism of gas detection depends on the design and structure of the photonic crystal. For example, some photonic crystal sensors utilize a resonant cavity design, where the adsorption of gas molecules shifts the resonant wavelength of the cavity. Other designs may rely on the changes in the photonic bandgap of the material, which can be detected using spectroscopic techniques.

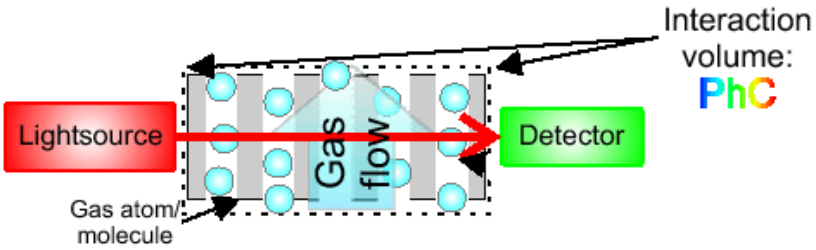

Figure. III. 1 Typical scheme of the gas detection system based on photonic crystals

III. 3. Mathematical background and proposed design

III. 3.1. Mathematical background

In our work, the plane wave expansion (PWE) method is used for photonic crystal modeling in order to determine photonic band gaps (TE and TM). The Finite-Difference Time-Domain FDTD method is used to solve Maxwell's equations by using Rsoft software. The proposed sensor is meshed with tiny grids (Δx, Δy). The grids size are selected with different values in the FDTD solution. Since the boundary conditions at the spatial boundaries of the computational domain must be carefully considered, the PML (perfectly matched layer) of one spatial unit thickness surrounding the simulated area absorbs the fields leaving the simulated region to implement reflections [1,2]. The propagation of light in a PhC biosensor is obtained by solving Maxwell's electromagnetic equations as follows [3]:

$$\nabla \times \left(\frac{1}{\varepsilon}\nabla \times H\right) = \left(\frac{\omega}{c}\right)^2 H \qquad (1)$$

Where ε is the permittivity, H is the magnetic field, ω is the frequency and C is the speed of light.

In this work, to obtain a stable simulation, one must adhere to the courant condition which relates the spatial and temporal step size [4] [5]:

$$C\Delta t < \frac{1}{\sqrt{(1/\Delta x^2 + 1/\Delta y^2 + 1/\Delta z^2)}} \qquad (2)$$

In the band structure computation of a PhC, dispersion relation is calculated by PWE Method. It is necessary to solve the eigen- problem formulated for the Helmholtz equation inside infinite periodic structure In order to obtain the dispersion relation, which is given below [6]:

$$\hat{\theta} H = \left(\frac{\omega^2}{c^2}\right) H \quad (3)$$

Where

$$\hat{\theta} = -\left(\frac{\partial}{\partial x}\right)\left(\frac{1}{\epsilon(x)}\right)\left(\frac{\partial}{\partial x}\right) \qquad (4)$$

(x) is the periodic dielectric function.

The optical RI of a medium is a vital optical parameter in explaining light-matter interactions. In this work, we will utilize substantial parameters to measure the overall performance of the biosensor Sensitivity (S) and Figure of merit (FoM).

They are calculated as follows[7]:

$$S = \frac{\Delta\lambda_0}{\Delta n_{analyte}} = \frac{\Delta\lambda_0}{\Delta n} \left(\frac{nm}{RIU}\right) \quad (5)$$

$$FoM = \frac{S}{(FWHM)} (RIU^{-1}) \quad (6)$$

Where $\Delta\lambda_0$the amount of variation in the resonant wavelength, Δn denotes the amount of variation in the refractive index and FWHM represents full width at half maximum (FWHM).

Figure of merit is also proportional to the quality factor (Q), where

$$Q = \frac{\lambda_0}{FWHM} \quad (7)$$

III. 3.2. The basic structure of the proposed gas sensor

The 2D-CP device consists of air holes (nair = 1) engraved on a silicon membrane with a refraction index(n_{Si} = 3.42), with the number of holes in the directions X and Z is 22×23. The distance between the center of two adjacent holes is 1.1nm which is called the grid constant and indicated by 'a' (periodicity). The radius of the hole r=a*0.29 µm.

Parameters	**Values**
Radius	0.29 x a µm
Network constant (a)	1.1 µm
Hole refraction index (Air)	1
Bottom refraction index (Si)	3.42
Platform Dimensions	22x23

Table III. 1Parameters of the sensors used in this work

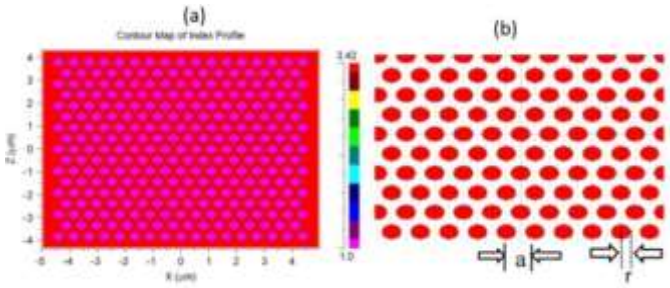

Figure. III. 2 (a) Index profile, (b) Scheme illustrates the geometric parameters of a 2D photon crystal

III. 3. 3. Gas sensors based on waveguide coupled with cavity

a- Creation of the overall structure

In this part, we used the Rsoft CAD simulation software to create our proposed structure (Figure III.3). To customize network settings; on click The global edit arrangements button that allows you to define network properties. (Figure. III.4 (a)). Figure III.4 (b) present the 'Symbol table editor' window that allows us to change the geometric parameters as well as the simulation parameters.

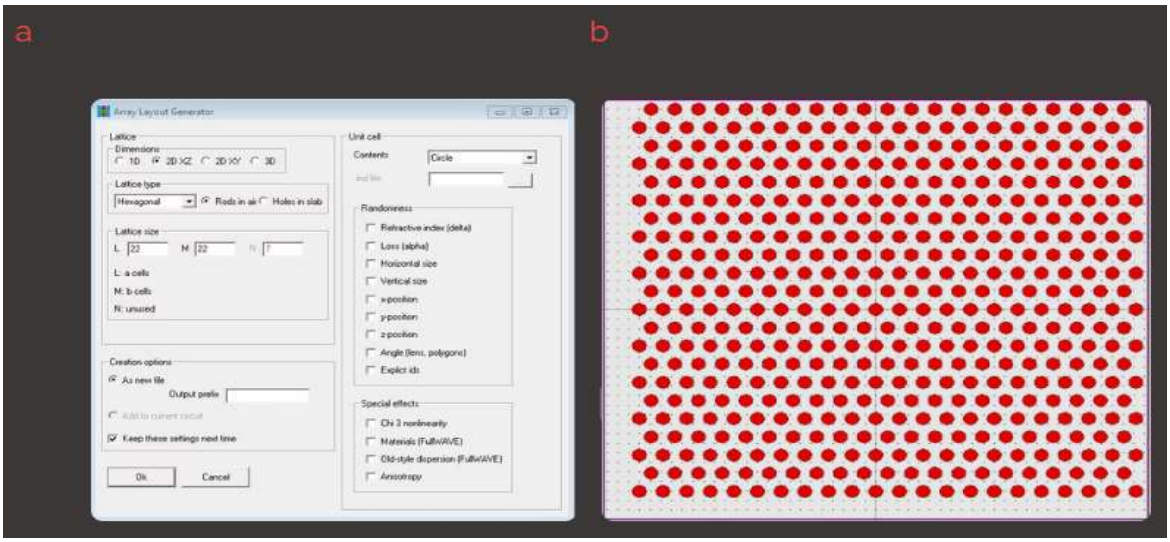

Figure. III. 3(a) Array layout generation, (b) network presentation

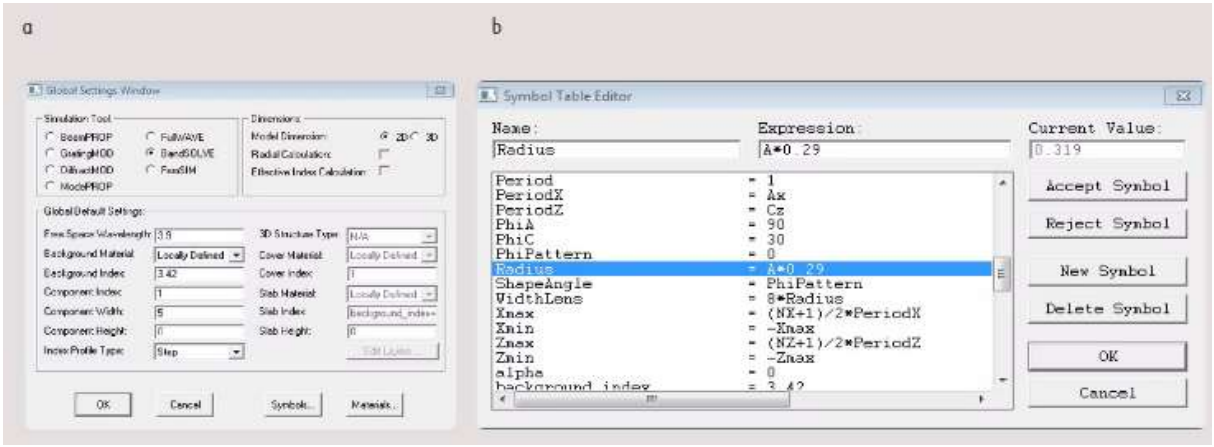

Figure. III. 4(a) Global Arrangements, (b) Symbol Publisher Table.

b- Study of the Forbidden band

Initially, we used RSoft's BandSOLVE module based on the 2D-PWE to determine Photonic banned bands (TE et TM).

Using the PWE method, the host structure's photonic band diagram has been calculated. the results shows that there are two normalized band gapsa aps in TM polarization mode (Figure. III.5).

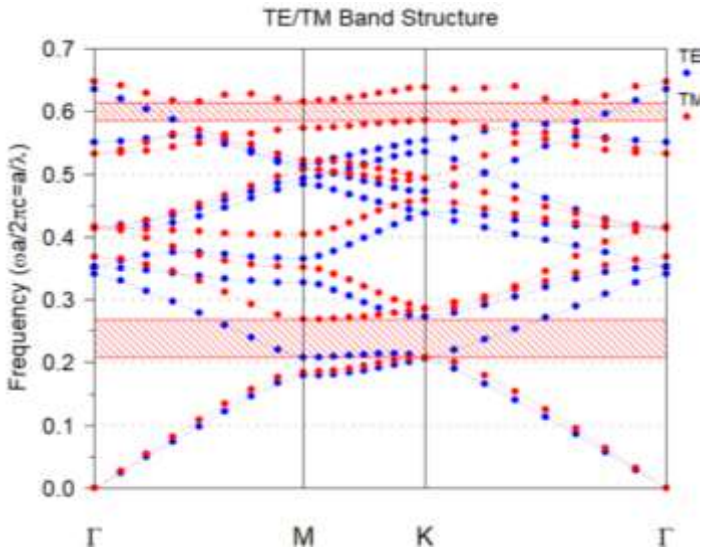

Figure. III. 5 photonic band diagram of the host structure

Another calculation allows the calculation of transmission as a function of wavelength in TM polarization; using the finite-difference time-domain (FDTD) method . This simulation makes it possible to plot the spectrum of the same photonic bandgap. Figure III.6 shows the spectrum for the triangular structure which has the widest PBG (Photonic band gap) in TM mode.

During the simulation process, the light source was positioned in the input line defect waveguide head, as for the monitor, it was placed at the end of the output line waveguide. The normalized central frequency of Gauss pulse source is centered around a/3.9.

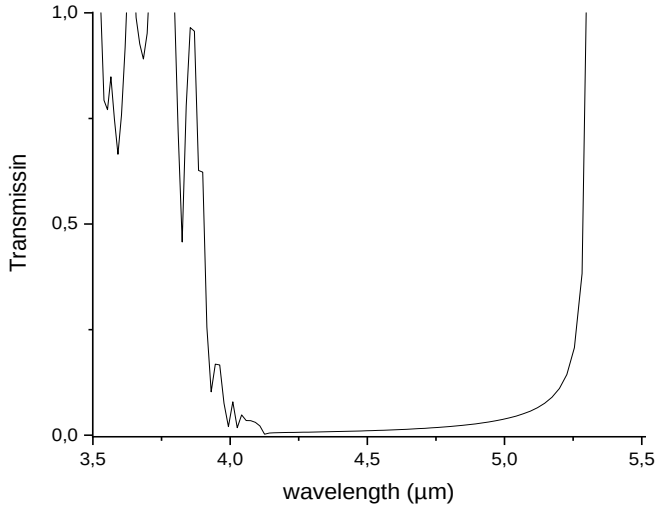

Figure. III. 6 Transmission spectra of the host stucture for TM polarisation.

Forbidden bands		Frequency range	Wavelength range (µm)
TM	**Bande1**	**0.58483≤(f=a/λ)≤0.61453**	**1.78998 ≤ λ ≤ 1.88088**
	Bande2	**0.20736≤(f=a/λ)≤0.2681**	**4.1029 ≤ λ ≤5.30478**

Table III. 2 Range of forbidden bands

c- Creation of waveguide

The waveguide is formed by removing a row of holes in the ΓK direction from the triangular grid (Figure. III.7 (a)). Initially, the grid parameters are given as follows.as follows: Triangular Array of air holes with periodicity a and hole's radius r. The Gaussian launch is placed at the input end of waveguide W1, and the monitor is located at the end of the output waveguide W1

to obtain transmission spectrum spectrum data. Figure. III.7 (b) shows the transmission spectra of the output of the waveguide.

a

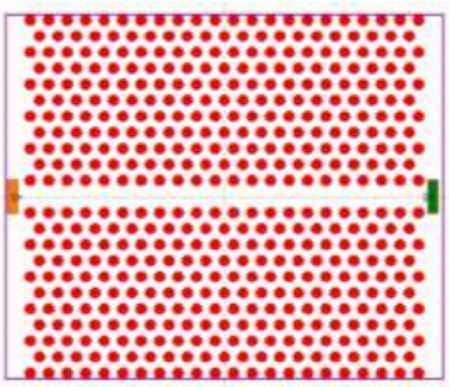

b

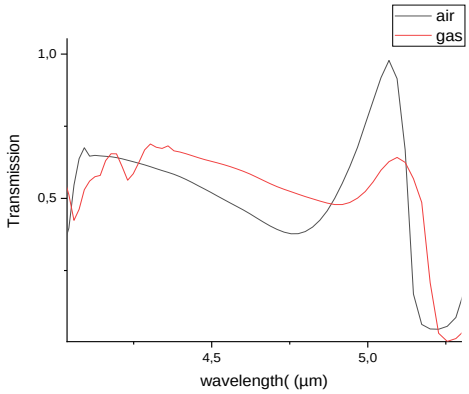

Figure. III. 7 (a) PhC waveguide design formed by omitting a line of air holes. (b) the transmission spectra.

d- Gas sensor based on a guide-cavity coupling

The schematic representation of the first proposed structure is shown in Figure III.8a, the proposed cavity is formed by inserted an air slot and six air holes in the centre of the waveguide with solt width is (Z-slot) and slot length (X- slot) .

a

b

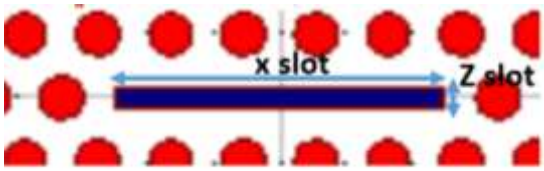

C

Figure. III. 8 (a) The proposed design of toxic gas sensor. (b) Schematic illustration of the geometric parameters of the central cavity. (c) Coupled-cavity systems for the realization of resonant effect.

III.4. Results and discussions

III.4.1 Study of proposed sensor

In order to acquire a new miniature photonic crystal toxic gas sensor with high sensitivity and FOM, a resonance-based device is proposed. The toxic gas sensor consists of a coupled waveguide with slot resonator with three holes on both sides. The geometric parameters of the structure are as follows: Xslot=460nm, Zslot=30nm, $r = 0.29 \times a$ nm and n_{trou}=1 $n_{subsrat}$=3.42 .

The the numbers of holes on both sides, values of Xslot and Zslot was chosen to ensure the effectiveness of the coupling region between the central resonator, the input waveguide and the output waveguide.

In this section, the numerical results due to the interaction of incident waves with our designed sensor are presented. In order to understand the effect of the slot coupled with waveguide , the simulated transmission spectra are numerically calculated by the 2D-FDTD method and given in figure.III.9. Multipe resonance modes can be generated based on this design. When the slot central resonator is inserted into the waveguide, destructive interference between the guided mode (supported by the waveguide) and resonant modes (created by the central slot) will occur, resulting in two sharp resonances in the transmission spectrum (λ_{M1res}=5.220291µm, λ_{M2res}=5.336174µm,)

As shown in Figure. 9a, the transmission of the resonant peaks (T_{peak}) are respectively 95% and 87%. The transmission spectrum is given in Figure. 9a, exhibiting resonances line shapes with strong sharp profiles. Approximately the resonances, the transmission undergoes a transition between 0% and 95 %, meaning the constructive and destructive interferences are located close to each other. This phenomenon is due to the rapid variation of the phase along the localized (resonance-assisted) pathway compared to the background pathway. The qualilty factor Q of the two resonance modes are3.8×10^6 and1.58×10^6. They has the FWHM at -3db 0.00309µm for the first mode, 0.00367 µm for the second mode.

a

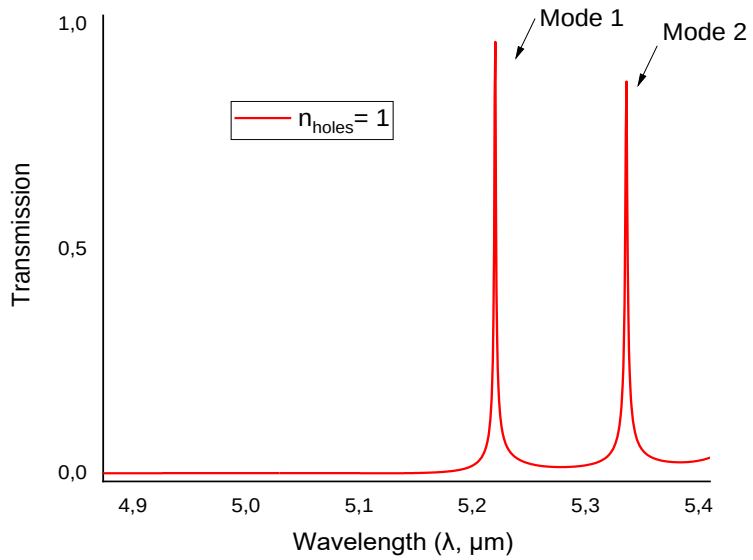

b

λ_{M1res}=5.220291µm

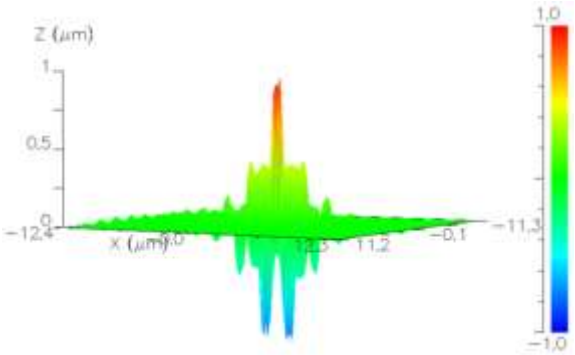

c

λ_{M2res}=5.336174µm

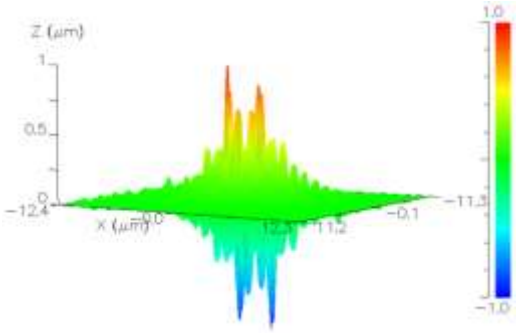

d

λ_{M2res}=5.336174µm

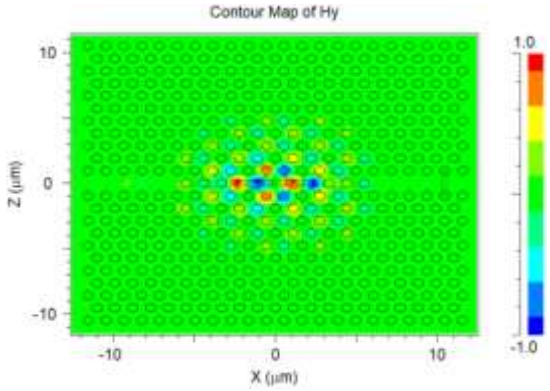

Figure. III. 9(a) Transmission spectra of the coupled system, (b, c) The 3D distributions of magnetic fields (|H| at different resonant wavelength (Mode 1 and 2), (d) The 2D distributions of magnetic fields (|H| of the second Mode

To better understand, Figures 9b-d illustrate the magnetic field (| Hy |) distribution for the proposed sensor at the resonances wavelength λ_0 of 5.220291µm and 5.336174µm. It can be seen that the magnetic field confined in slot resonator. For this reason, we have investigated the effect of varying the geometric parameter of the slot to optimize the detection criteria.

The peaks are sensitive of the alteration of the refractive index around the surface of distribution (| Hy |). By varying the refractive index of holes from n = 1 to n = 1.002, can induce a shift of the resonance spectrum. The sensitivity is calculated by varying RI (Δn = 0.002) is 545.5nm/RUI for the first mode and 285 nm/RUI for the second mode.

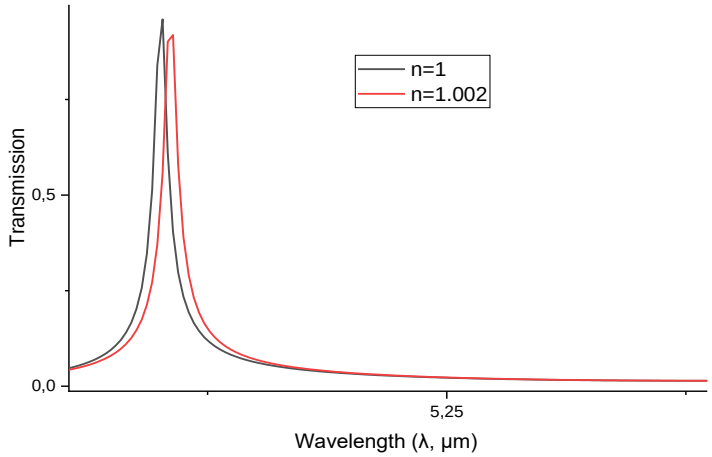

Figure. III. 10Transmission spectra of sensor varying the refractive index of holes from n = 1 to n = 1.002

III.4.2 Slot geometric parameters effect

To study and enhance the performance of the proposed toxic gas sensor, we fixed the value of the slot width Z-slot (Z-slot =0.3µm) and varied the slot length (X-slot) from 4.2 to 4.8 µm with a step of 0.02. The shift of the resonant modes, transmission and sensitivity of this gas sensor obtained for different X-slot are simulated and presented in figure. III.11. It is very clear that the higher transmission and sensitivity are for X-slot=4.4µm.

Table III.3 show the variation of the FWHM , quality factor and FoM as a function of the variation of X-slot . It is very clear that for the two modes the FWHM values are low, which is very desirable for measuring the refractive index variation. The quality factor Q varied between $1.51*10^6$ and $1.2*10^7$.

a

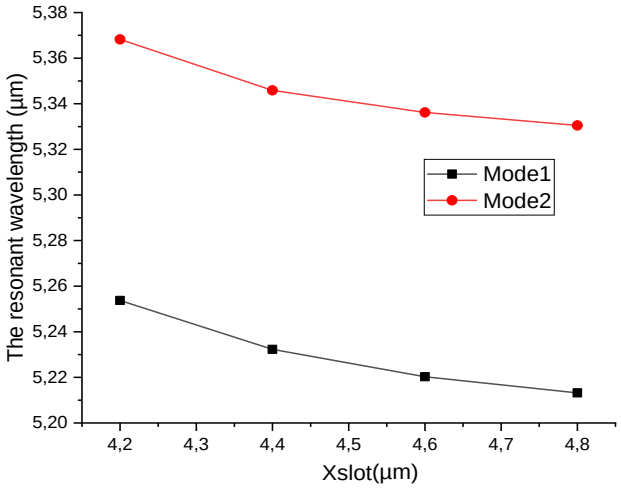

b

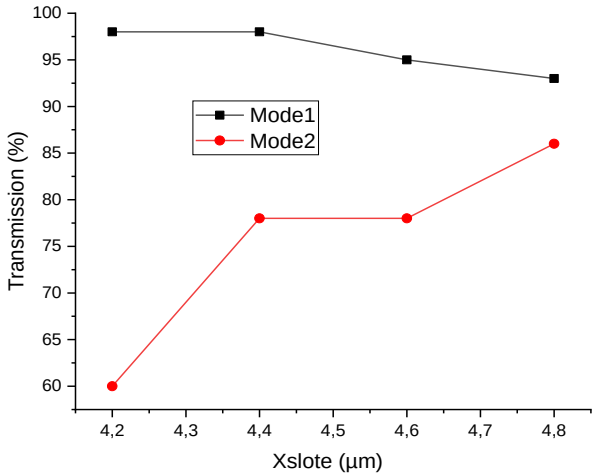

c

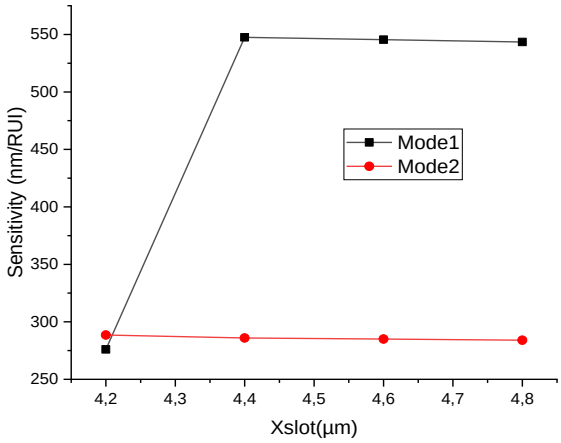

Figure. III. 11 The variation of the resonant wavelenght (a), transmission (b) and sensitivity (c) as a function of the change of X-Slot.

Xslot (µm)	FWHM (µm)		$Q = \frac{\lambda_{res}}{FWHM}$		$FoM = \frac{S}{(FWHM)}(RIU^{-1})$	
	M1	M2	M1	M2	M1	M2
4.2	0.00262	0.00386	$1.2*10^7$	$1.58*10^6$	$6.31*10^5$	$8.51*10^4$
4.4	0.00203	0.0025	$5.65*10^6$	$1.51*10^6$	$5.91*10^5$	$8.08*10^4$
4.6	0.00309	0.00367	$3.81*10^6$	$1.58*10^6$	$3.98*10^5$	$8.46*10^4$
4.8	0.00289	0.00302	$1.90*10^6$	$2.87*10^6$	$1.98*10^5$	$1.53*10^5$

Table III. 3 Variation of FWHM, Quality factor and FoM as a function of the change of X-Slot

In this section, we the the same senario, we fixed the value of the slot width X-slot (X-slot =4.4µm) and varied the slot length (Z-slot) from 0.6 to 0.9 µm with a step of 0.05.

The shift of the resonant modes, transmission and sensitivity of this gas sensor obtained for different Z-slot are simulated and presented in Figure. III.12. It is very clear that the higher transmission and sensitivity are for Z-slot=0.7µm

Table III.4 show the variation of the FWHM , quality factor and FoM as a function of the variation of Z-slot . It is very clear that for the two modes the FWHM values are low, which is very desirable for measuring the refractive index variation. The quality factor Q variedbetween $1.48*10^6$ and $1.07*10^7$.

a

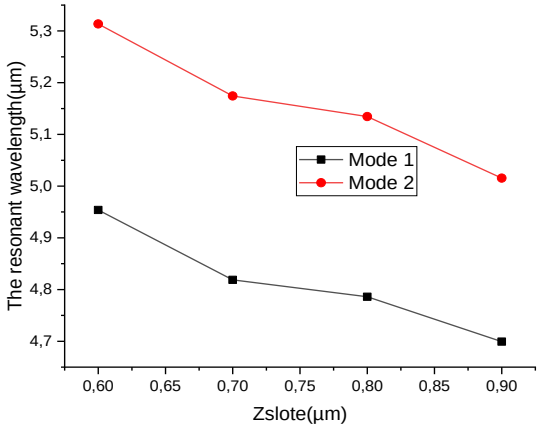

b

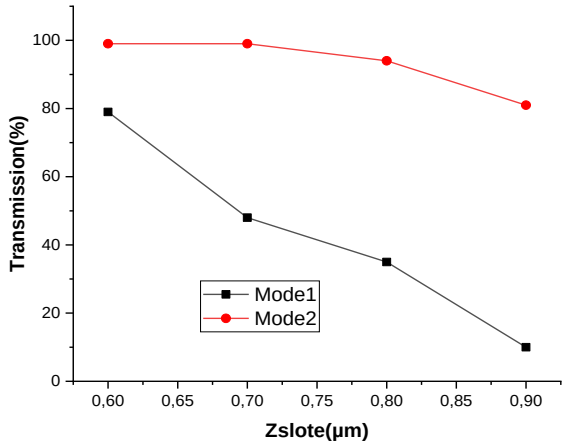

c

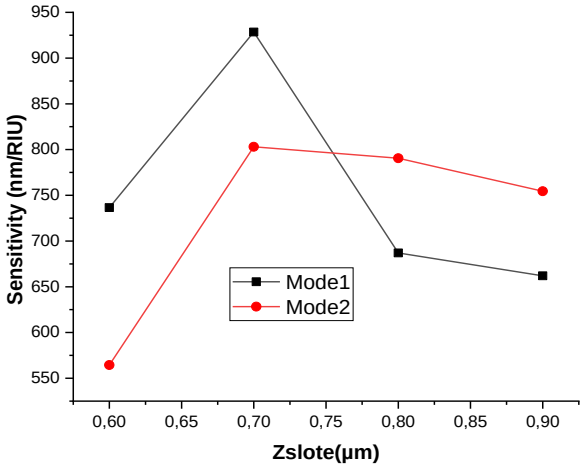

Figure. III. 12The variation of the resonant wavelenght (a), transmission (b) and sensitivity (c) as a function of the change of Z-Slot.

Zslot (µm)	FWHM (µm)		$Q = \frac{\lambda_0}{FWHM}$		$FoM = \frac{S}{(FWHM)}(RIU^{-1})$	
	M1	M2	M1	M2	M1	M2
0.9	$4.3709*10^{-4}$	0.00339	$1.07*10^{7}$	$1.48*10^{6}$	$1.51*10^{6}$	$2.23*10^{5}$
0.8	$9.2571*10^{-4}$	0.00354	$5.17*10^{6}$	$1.45*10^{6}$	$7.42*10^{5}$	$2.23*10^{5}$
0.7	0.00137	0.00337	$3.52*10^{6}$	$1.53*10^{6}$	$6.78*10^{5}$	$2.38*10^{5}$
0.6	0.00275	0.00186	$1.80*10^{6}$	$2.86*10^{6}$	$2.68*10^{5}$	$3.03*10^{5}$

Table III. 4 Variation of FWHM, Quality factor and FoM as a function of the change of Z-Slot

III.4.3 Optimized sensor

Us we mention perviously the resonant modes are sensitive of the alteration of the refractive index around the surface of distribution (| Hy |). So,To enhance the transmission and the sensitivity of the sensor, we inser an air hole in the centre of the slot with raduisRC.

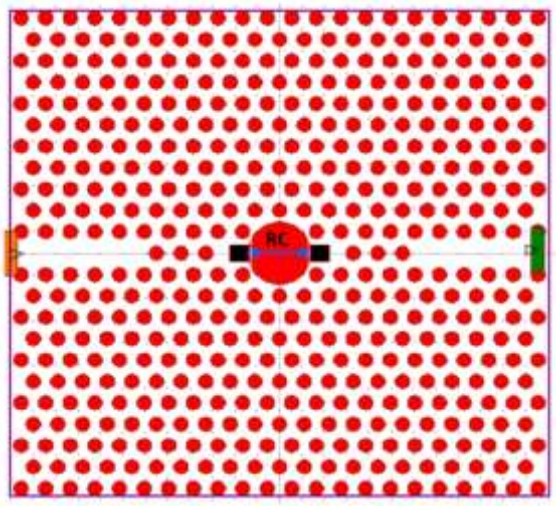

Figure. III. 13optimized sensor

The variation of the transmission and sensitivity as a function of the variation of RC are simulated and presented in figure III. 14, It is very clear that the higher transmission and sensitivity are for RC=R*4.4 µm

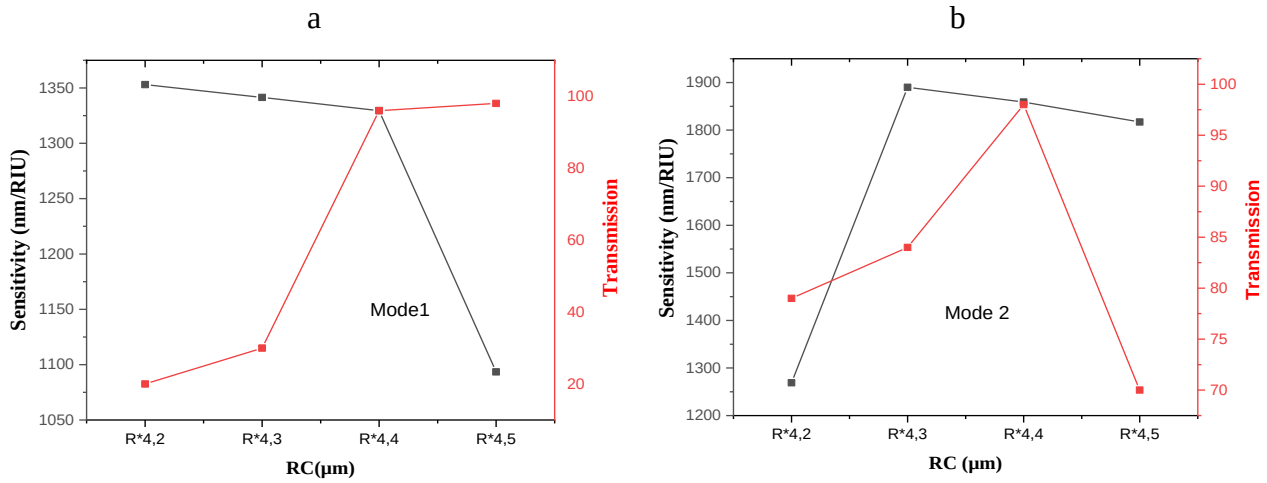

Figure. III. 14The variation of the transmission and sensitivity as a function of the change of RC, (a) Mode 1, (b) Mode 2.

III.4.4 Application: Toxic gaz sensor

Acetylene is an organic gas that contributes to the formation of photochemical oxidants and predicted warming of the atmosphere. It is therefore classified as a Volatile Organic Compound (VOC). Specific legal requirements on VOC emissions reporting may exist depending on the country.

Acetylene gas, chemically represented as C_2H_2 (n = 1.000579) [8], is a colorless, highly flammable gas with a distinct garlic-like odor. It's produced through the reaction of calcium carbide with water. Acetylene is commonly used in oxy-fuel welding and cutting due to its high flame temperature, which can reach up to 3,500°C (6,330°F) in oxygen-rich environments. It's also utilized in various industrial processes, such as in the synthesis of organic compounds and as a precursor in the production of plastics and chemicals. However, due to its highly explosive nature, it requires careful handling, storage, and transportation.

In this section,we assumed that the air holes (n = 1,000265) were completely infiltrated with Acetylene(C_2H_2, n = 1,000579). Figure. III.15 shows the transmission spectrum of the proposed structure corresponding to the infiltration calculated by the FDTD method. We observe a shift of 0,443nm in the resonant wavelength, for the first mode, which gives a sensitivity of 1410,8 nm/RIU.

We also observe a shift of 0,465 nm in the resonant wavelength, for the second mode, which gives a sensitivity of 1480,89nm/RIU.

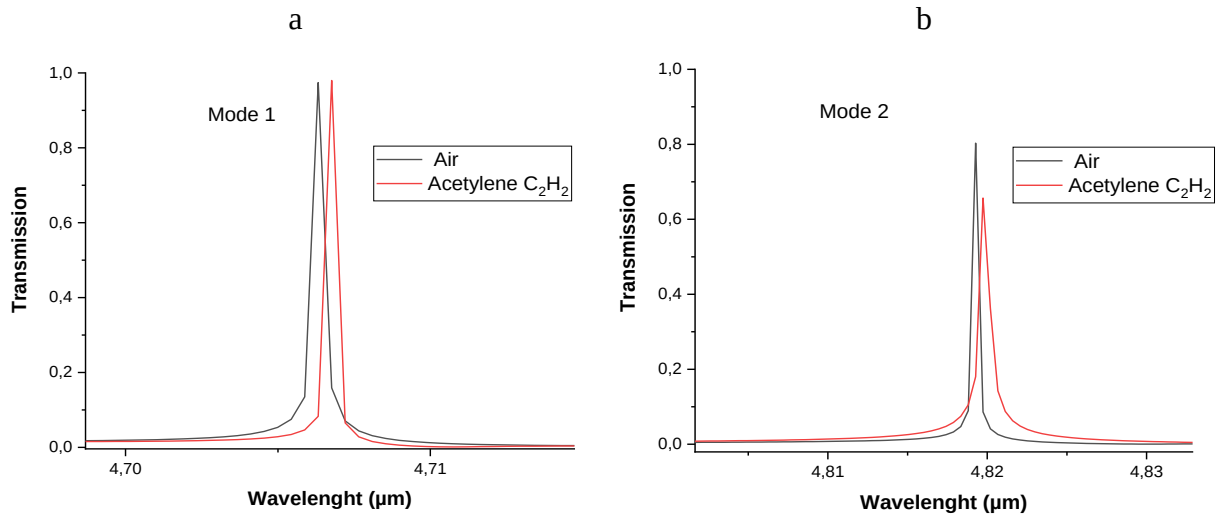

Figure. III. 15Transmission spectrum of the optimized Toxic gas sensor, (a) Mode 1, (b) Mode 2

III.5. Conclusion

In this work, we propose a PhC-based sensor for Toxic gas detection based on refractive index variation. The proposed device is consists of a waveguide coupled slot resonator. The FDTD simulation results show that for small changes in the refractive index (RI) of the input samples (infitration of gas in holes), there is a significant shift in the resonance wavelength. This means that the designed toxic gas sensor is highly sensitive to small RI variations. Our optimized optical gas sensor can offer high sensitivity and figure of merit (FOM) that is comparable to existing sensors. designed gas ensor is very sensitive even to small RI variations. Our optimized optical toxic gas sensor can offer high sensitivity and quality factor that is competitive with current sensors.

References

[1]Harhouz, A., & Hocini, A. (2015). Design of high-sensitive biosensor based on cavity-waveguides coupling in 2D photonic crystal. *Journal of Electromagnetic Waves and Applications*, *29*(5), 659-667.

[2]Hocini, A., Moukhtari, R., Khedrouche, D., Kahlouche, A., & Zamani, M. (2017). Magneto-photonic crystal microcavities based on magnetic nanoparticles embedded in silica matrix. *Optics Communications*, *384*, 111-117.

[3]Yee, K. S. (1966). Numerical solution of initial boundary value problems involving Maxwell's equations in isotropic meida. *IEEE Trans. Antennas Propagat*, *14*(5), 1327-1333.

[4]A. Taflove and M. Brodwin. (1975) Numerical solution of steady-state electromagnetic scattering problems using the time-dependent Maxwell's equations, IEEE transactions on microwave theory and techniques, vol. 23(8), 623-630,

[5]K. Karls and J. Raymond. (1993) The Finite Difference Time Domain Method for, Boca Raton: CRC Press.

[6]Chhoker, P., and S. Bajaj. "Analysis of photonic band structure in 1-D photonic crystal using PWE and FDTD Method." *IJISET Int J Innov Sci Eng Technol* 2 (2015): 883-887.

[7]Hajshahvaladi, L., Kaatuzian, H., & Danaie, M. (2021). Design of a hybrid photonic-plasmonic crystal refractive index sensor for highly sensitive and high-resolution sensing applications. *Physics Letters A*, *420*, 127754.

[8]Kassa-Baghdouche, L., & Cassan, E. (2018). High efficiency slotted photonic crystal waveguides for the determination of gases using mid-infrared spectroscopy. Instrumentation Science & Technology, 46(5), 534-544.

General Conclusion

Photonic crystals are materials characterized by periodic variations in refractive index across one, two, or three spatial dimensions at the scale of wavelengths. They represent a novel class of materials akin to semiconductors, with photons organized into transmission bands separated by photonic band gaps. This similarity enables the manipulation of light using photonic crystals, opening avenues for diverse research and applications. The advancement of this material promises exploration into new realms of study and a wide array of practical uses.

The main objective of this master thesis is the design of new structures based on two-dimensional slotted-waveguide coupled-cavity photonic crystals (2D-PhCs) for environmental monitoring applications operating in the mid-IR, to enhance their performance.

Firstly, we have presented the application of optical nanosensors in environmental monitoring, as the nanophotonic sensors are a promising tool in addressing complex environmental challenges.

Then, we have presented a general reminder of the fundamental concepts related to photonic crystals and their photonic properties where we have demonstrated the importance of using photonic crystals as a sensor. Special emphasis is placed on the study of refraction index (RI) biosensors based on two-dimensional photonic crystals, where the refractive index is set as a parameter to design optical sensor devices using photonic crystals giving general characteristics and working principles of the different types of sensors and their applications.

In this work, we have successfully designed and simulated a novel 2D-PhC platform for environmental monitoring. The suggested 2D-PhC Mid-IR sensor can generate two different modes and may differentiate between several different analytes using the modules developed by the RSoft-CAD software ideally suited to the design of the 2D photonic circuits, BandSOLVE (based on the PWE method), and FullWAVE (based on the FDTD method), respectively, which are based on direct resolution of Maxwell's equations. Our results show that the suggested sensor has a high sensitivity of S=1 410,8 nm/RIU, an amazing Q-factor up to $1.2*10^{7}$, an ultra-high FOM of $1.51*10^{6}$ RIU–1, and an incredible detection limit of 10^{-4} RIU. The sensing features of the biosensor are achieved by varying the refractive index of the analyte.

Design and simulation of photonic crystal sensor based on waveguide coupled cavity for environmental monitoring

Abstract: The environment is crucial to a healthy lifestyle and the continued existence of life on Earth. Nonetheless, throughout the past several years, there has been a significant increase in environmental pollution due to the world population rise along with technological improvement. For these reasons, numerous new sensors and methods have been developed to effectively identify different types of environmental pollution. Among all the methods proposed for environmental monitoring, photonic crystal devices have demonstrated great potential in sensing applications due to their high sensitivity to changes in refractive index, visual identifiability, room- temperature operability and easy portability. Recently, integrated mid-infrared (mid-IR) photonics have gained considerable attention due to the fact that most of the gases have their characteristic absorption peak in the mid-IR range, and as a result, Mid-IR photonic crystal can serve as an ideal, with enormous potential for new applications in optical interconnects and sensing. In this work, the proposed device is simulated using Plane Wave Expansion (PWE) method and Finite-Difference Time-Domain (FDTD) algorithm. The high performance and simple design of the proposed sensor make it a suitable candidate for environmental monitoring.
Keywords: toxic gas sensor, Photonic crystals, waveguide, 2D CP sensor, FDTD,

Résumé : L'environnement est essentiel à un mode de vie sain et à la poursuite de la vie sur Terre. Néanmoins, au cours des dernières années, la pollution de l'environnement a augmenté de manière significative en raison de l'accroissement de la population mondiale et des progrès technologiques. C'est pourquoi de nombreux nouveaux capteurs et méthodes ont été mis au point pour identifier efficacement les différents types de pollution environnementale. Parmi toutes les méthodes proposées pour la surveillance de l'environnement, les dispositifs à cristaux photoniques ont démontré un grand potentiel dans les applications de détection en raison de leur grande sensibilité aux changements d'indice de réfraction, de leur identifiabilité visuelle, de leur fonctionnement à température ambiante et de leur facilité de transport. Récemment, la photonique intégrée dans l'infrarouge moyen (IR moyen) a fait l'objet d'une attention considérable en raison du fait que la plupart des gaz ont leur pic d'absorption caractéristique dans l'IR moyen et que, par conséquent, le cristal photonique IR moyen peut servir de solution idéale, avec un potentiel énorme pour de nouvelles applications dans le domaine des interconnexions optiques et de la détection. Dans ce travail, le dispositif proposé est simulé à l'aide de la méthode d'expansion des ondes planes (PWE) et de l'algorithme FDTD (Finite-Difference Time-Domain). Les performances élevées et la conception simple du capteur proposé en font un candidat approprié pour la surveillance de l'environnement.
Mots clés : capteur de gaz toxique, Cristaux photoniques, guide d’onde, capteur à CP 2D, FDTD,

الملخص : البيئة أمر بالغ الأهمية لنمط حياة صحي واستمرار الحياة على الأرض. ومع ذلك، وخلال السنوات العديدة الماضية، حدثت زيادة كبيرة في التلوث البيئي خلال السنوات العديدة الماضية بسبب ارتفاع عدد سكان العالم إلى جانب التطور التكنولوجي. ولهذه الأسباب، تم تطوير العديد من أجهزة الاستشعار والطرق الجديدة لتحديد أنواع مختلفة من التلوث البيئي بشكل فعال. ومن بين جميع الطرق المقترحة للرصد البيئي، أظهرت أجهزة الكريستال الضوئي إمكانات كبيرة في تطبيقات الاستشعار بسبب حساسيتها العالية للتغيرات في معامل الانكسار وإمكانية التعرف البصري وقابلية التشغيل في درجة حرارة الغرفة وسهولة حملها. في الآونة الأخيرة، اكتسبت ضوئيات منتصف الأشعة تحت الحمراء المدمجة (منتصف الأشعة تحت الحمراء) اهتمامًا كبيرًا نظرًا لحقيقة أن معظم الغازات لها ذروة امتصاص مميزة في نطاق منتصف الأشعة تحت الحمراء، ونتيجة لذلك، يمكن أن تكون البلورات الضوئية متوسطة الأشعة تحت الحمراء بمثابة نموذج مثالي، مع إمكانات هائلة للتطبيقات الجديدة في التوصيلات البينية البصرية والاستشعار. في هذا العمل، تمت محاكاة الجهاز المقترح باستخدام طريقة توسيع الموجة المستوية (PWE) وخوارزمية المجال الزمني المحدود الاختلاف (FDTD).إن الأداء العالي والتصميم البسيط لجهاز الاستشعار المقترح يجعله مرشحًا مناسبًا للرصد البيئي.
الكلمات المفتاحية: كاشف الغازات السامة ,بلورات ضوئية ، دليل موجي ، ، مستشعر ثنائي ألبعاد CP ، FDTD،